

nomic and subgenomic HCV-1b replicons [15, 16]. Even though the precise mechanism has not been defined, these agents may attenuate HCV replication through the destruction of lipid rafts, according to their pharmacological actions. If this is the mechanism, sphingomyelin, the remaining and essential component of lipid rafts, might play a role in HCV replication. With this in view, recent studies have demonstrated that a sphingomyelin synthesis inhibitor attenuated the replication of a subgenomic HCV-1b replicon in cultured cells [17] and the replication of genomic HCV-1 in a chimeric mouse model [18]. However, investigation of anti-HCV activity in these agents has been limited to genotype 1 HCV, and the combined effect of these agents has not been determined. If they do not target the HCV structure itself but exert their antiviral activity through destruction of the host's lipid raft, it would be plausible to speculate that they might be effective irrespective of the viral isolate, and the combined effect of these agents might be additive or synergistic.

In the present study, we investigated the role played by the sphingomyelin synthesis pathway and the mevalonate pathway in HCV replication, using a subgenomic HCV-1b replicon and the particle-producing cell culture HCV 2a model of JFH-1 HCV [19].

## MATERIALS AND METHODS

**Cell culture and HCV replicon.** The human hepatoma cell lines Huh7 and Huh7.5.1 [20] were maintained in Dulbecco's modified Eagle's medium (Sigma) supplemented with 10% fetal calf serum at 37°C in 5% CO<sub>2</sub>. The subgenomic HCV replicon used was derived from Rep-Feo (genotype 1b) [21, 22], and a full-length genomic HCV RNA was derived from genotype 2a JFH-1 HCV [19]. Subgenomic or genomic HCV RNA was synthesized from replicon cDNA-harboring plasmids (pRep-Feo and pJFH-1) by means of T7 polymerase (RiboMax Large Scale RNA Production System; Promega) and transfected into these cells. For the subgenomic replicon, cell lines stably expressing the replicon were established (Huh7/Rep-Feo) in the presence of 500 µg/mL G418.

**Reporter plasmids and luciferase assay.** pISRE-TA-Rluc expressing the *Renilla* luciferase reporter gene under control of the IFN-stimulated response element (ISRE) was constructed by replacing the firefly luciferase gene with the *Renilla* luciferase gene of pISRE-TA-Luc, purchased from Invitrogen. Luciferase activity was quantified using the Bright-Glo or Dual-Luciferase assay system (both from Promega) and a luminometer (AB-2250; ATTO). Assays were performed in triplicate, and the results were expressed as mean ± SD percentages of the control values. QuantiLum recombinant luciferase (Promega) was used as the positive control for the analysis.

**Reagents.** The reagents used included myriocin (Biomol), IFN-α 2b (Santa Cruz Biotechnology), phytosphingosine hydrochloride (Sigma), 2-hydroxypropyl-β-cyclodextrin (2-HP-β-CyD; Sigma), and simvastatin (Cosmobio).

**Northern blotting.** Total cellular RNA was extracted from cells by means of Isogen (Wako). The RNA was separated by denaturing agarose-formaldehyde gel electrophoresis and transferred to a membrane from a NorthernMax kit (Ambion). The membrane was hybridized with a digoxigenin-labeled probe that was specific for the nonstructural replicon sequence. The signals were detected in a chemiluminescence reaction by using a digoxigenin detection kit (Roche) and were visualized by using an LAS-1000 imaging system (Fuji Film).

**Western blotting.** Ten micrograms of total cell lysate was separated using NuPAGE 4%–12% Bis-Tris gel (Invitrogen) and was blotted onto an Immobilon polyvinylidene difluoride membrane (Roche). The membrane was incubated with an anti-core monoclonal antibody (MAB; Affinity Bioreagents), an anti-NS3 MAB (Virogen), an anti-NS5A MAB (gift from Burckstummer, Robert Koch Institute), or a anti-β-catenin MAB (Sigma). Detection was done in a chemiluminescence reaction (ECL; Amersham).

**Dimethylthiazol carboxymethoxyphenyl sulfophenyl tetrazolium (MTS) assays.** To evaluate cytotoxicity, MTS assays were performed using a CellTiter 96 Aqueous One Solution Cell Proliferation Assay (Promega), in accordance with the manufacturer's instructions.

**Thin-layer chromatography (TLC).** The lipid fraction of cells treated with myriocin was extracted using the method of Bligh and Dyer [23], and total lipids from the cells treated with myriocin were extracted with 3 mL of chloroform. The extracts were spotted onto silica gel TLC plates (Merck) and were chromatographed with chloroform-methanol-water (65:25:4 [vol/vol/vol]). The plate was visualized with a molybdenum spray.

**Real-time reverse-transcription polymerase chain reaction (RT-PCR).** TaqMan RT-PCR targeting the 5' untranslated region was used for the quantitation of intracellular genomic JFH-1 HCV RNA. The sequences of the sense and antisense primers and the TaqMan probe were 5'-TGCGGAACCGGTGAGTACA-3', 5'-CTTAAGGTTTAGGATTCGTGCTCAT-3', and 5'-(FAM)CAC-CCTATCAGGCAGTACCACAAGGCC(TAMRA)-3', respectively. The method has been described elsewhere [24].

**Short interfering RNA (siRNA) analysis.** The sequence encoding the LCB1 subunit of serine palmitoyltransferase (SPT) was selected as the target for siRNA (sense, 5'-AACAA-CAUCGUUUCAGGUCCU<sup>TT</sup>-3'; antisense, 5'-AGGGCCUG-AAACGAUGUUG<sup>TT</sup>-3'). siRNA targeting enhanced green fluorescent protein (GFP) was used as the negative control (sense, 5'-CUUACGCUGAGUACUUCGAT<sup>T</sup>-3'; antisense, 5'-UCG-AAGUACUCAGCGUAAT<sup>T</sup>-3'). (Underlined letters indicate deoxyribonucleotides.)

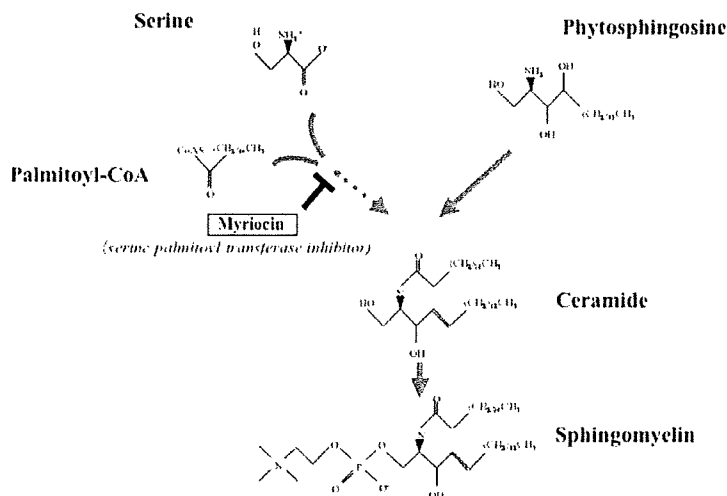


**Figure 1.** The sphingomyelin synthesis pathway. Serine palmitoyltransferase catalyzes the first committed step of sphingomyelin biosynthesis from serine and palmitoyl-coenzyme A (CoA). Myriocin inhibits the catalyzing activity of serine palmitoyltransferase. Phytosphingosine is known to work as a precursor of ceramide in both mammalian and fungal cells.

**Statistical analyses.** Statistical analyses were performed using Student's *t* test; statistically significant differences were defined as those for which  $P < .05$ .

## RESULTS

**Specific suppression of the replication of a subgenomic HCV-1b replicon by an inhibitor of sphingomyelin synthesis.** To clarify the role played by the sphingomyelin synthesis pathway in HCV replication, we added myriocin, a specific inhibitor of SPT that catalyzes the first committed step of sphingomyelin biosynthesis (figure 1), to the medium of Huh7/Rep-Feo cells. The luciferase activity, reflecting replication of the subgenomic HCV-1b replicon, dropped to 37% and 21% of the control at myriocin concentrations of 100 and 1000 nmol/L, respectively (figure 2A, upper panel), but myriocin did not cause toxicity to the cultured cells (figure 2A, lower panel). The result indicates that the decrease in HCV replication is due to a specific suppressive effect of myriocin and not to the cytotoxicity of myriocin. Northern hybridization analysis also demonstrated a substantial reduction of the subgenomic HCV replicon RNA in Huh7/Rep-Feo cells treated with myriocin in a dose-dependent manner (figure 2B). Similarly, Western blot analysis demonstrated a decrease in HCV NS5A after treatment with myriocin (figure 2C).

**No enhancement of ISRE promoter activity after myriocin treatment.** To determine whether the effect of myriocin in suppressing the subgenomic HCV replicon was associated with the activation of IFN-stimulated genes, the ISRE-*Renilla* luciferase plasmid was transfected into Huh7/Rep-Feo cells, and these cells were cultured with various concentrations of myriocin. As a positive control for the enhancement of ISRE reporter

activity, the ISRE-*Renilla* luciferase-transfected cells were cultured with IFN. Myriocin had no significant effect on ISRE promoter activity, whereas IFN significantly up-regulated ISRE activity (figure 2D, upper panel). In contrast, firefly luciferase activity in the Huh7/Rep-Feo cells, reflecting HCV replication, was inhibited by both IFN and myriocin in a dose-dependent manner (figure 2D, lower panel). These results demonstrate that the action of myriocin on HCV replication is independent of the IFN pathway.

**Decrease in the sphingomyelin content of Huh7 cells after myriocin treatment.** To clarify whether myriocin really inhibits the biosynthesis of sphingomyelin in Huh7 cells, we treated Huh7 cells with 100 nmol/L myriocin and analyzed the change in the cellular phospholipid composition by TLC. As demonstrated in figure 2E, the cellular sphingomyelin content decreased after myriocin treatment, but no significant change was observed in other cellular phospholipids.

**Restoration of HCV replication by addition of phytosphingosine.** To confirm that suppression of HCV RNA replication was due to depletion of sphingomyelin, we incubated replicon cells with phytosphingosine, a precursor of ceramide in mammalian and fungal cells, in the presence of myriocin. Treatment with phytosphingosine restored HCV replication in a dose-dependent manner (figure 2F, upper panel). On the other hand, phytosphingosine by itself did not have any effect on HCV replication (figure 2F, lower panel). This result indicates that inhibition of HCV replication was the direct result of depletion of sphingomyelin.

**Suppression of HCV replication by knocking down SPT with siRNA.** Next, we determined whether inhibition of SPT expression suppresses HCV replication by knocking down SPT with siRNA. As demonstrated in the upper panel of

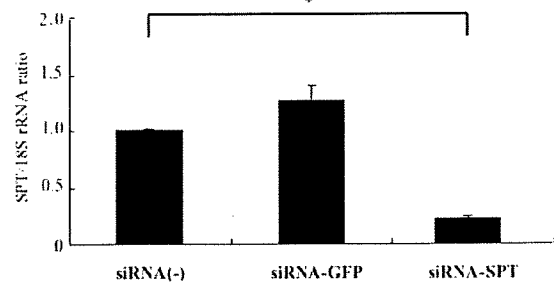
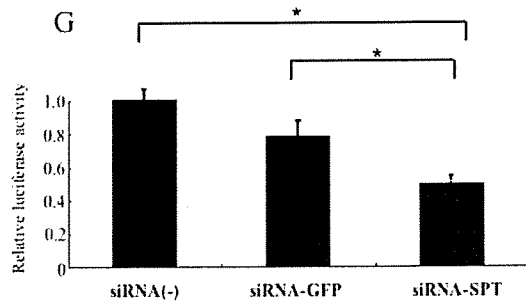
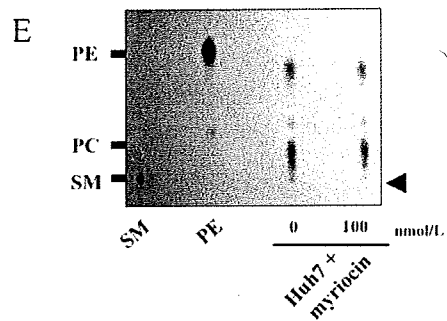
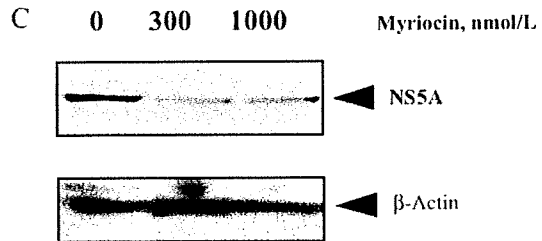
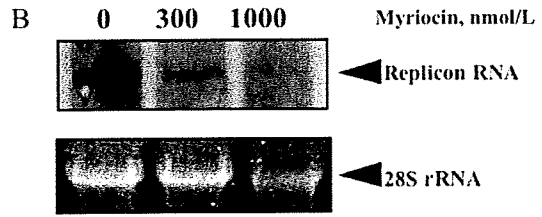
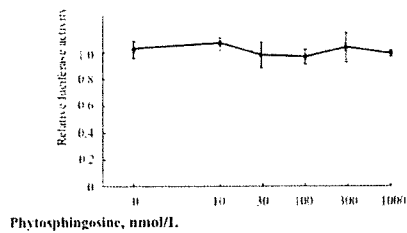
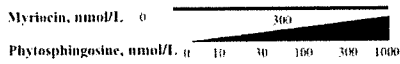
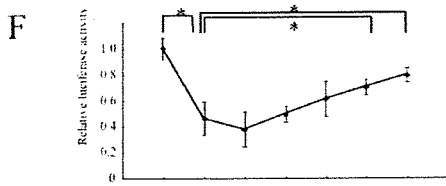
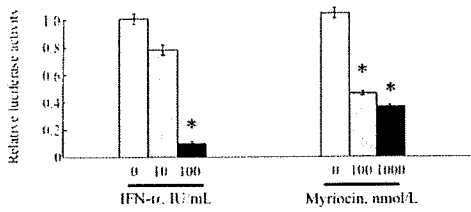
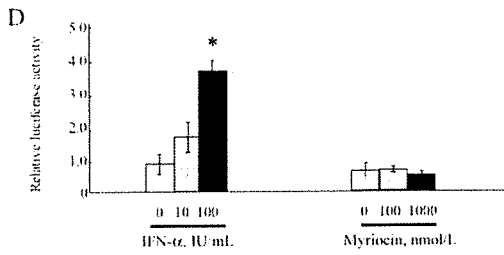
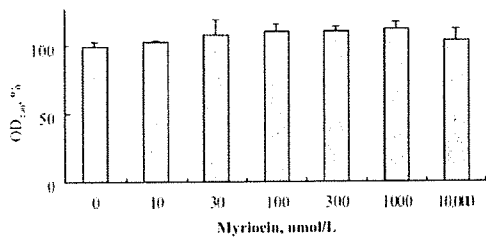
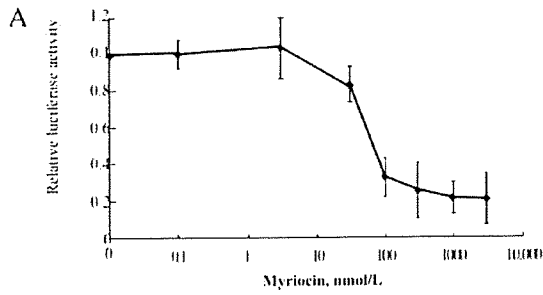


figure 2G, HCV replication was suppressed significantly by siRNA targeting SPT compared with no siRNA or siRNA targeting GFP (negative control). We confirmed with real-time PCR that the siRNA targeting SPT significantly decreased expression of SPT mRNA (figure 2G, lower panel). This result indicates that the SPT enzyme plays an important role in HCV replication.

**Inhibition of the replication of a subgenomic HCV-1b replicon by an HMG-CoA reductase inhibitor (simvastatin).** HMG-CoA reductase inhibitors have been reported to suppress replication of subgenomic and genomic HCV-1b replicons [15, 16]. Because cholesterol is another important component of lipid rafts, it may be speculated that depletion of cholesterol by HMG-CoA reductase inhibitors disrupts the lipid raft, affecting the ability of the HCV replicon to replicate in Huh7 cells. To confirm the effect of HMG-CoA reductase inhibitors on the subgenomic HCV-1b replicon, we examined the effect of simvastatin by means of Huh7/Rep-Feo cells. Cultures of Huh7/Rep-Feo cells with simvastatin at concentrations of 0–100  $\mu\text{mol/L}$  showed a dose-dependent reduction of the subgenomic HCV-1b replicon (figure 3, upper panel). The MTS assay showed that treatment with simvastatin had no toxic effect on Huh7/Rep-Feo cells in the dose range used (figure 3, lower panel). These results demonstrated that simvastatin specifically suppressed replication of a subgenomic HCV-1b replicon. However, because recent studies showed that statins suppress HCV replication through inhibition of geranylgeranylation of certain proteins rather than inhibition of cholesterol synthesis [15], we also

examined the effect on HCV replication of 2-HP- $\beta$ -CyD, an agent known to deplete cholesterol directly from membranes. As demonstrated in figure 4A, 2-HP- $\beta$ -CyD also suppressed HCV replication without cytotoxicity. To confirm that 2-HP- $\beta$ -CyD did not inhibit firefly luciferase activity nonspecifically rather than by suppressing HCV RNA, we incubated recombinant firefly luciferase with various concentrations of 2-HP- $\beta$ -CyD in the culture medium, and the medium was subjected to luciferase analysis. As demonstrated in figure 4B, 2-HP- $\beta$ -CyD did not affect luciferase activity. These results indicate that cholesterol itself plays an important role in HCV replication.

**Synergistic inhibitory effects of myriocin with IFN, simvastatin with IFN, and myriocin with simvastatin.** We carried out the following assay to determine whether myriocin and IFN have a synergistic inhibitory effect on HCV replication. Huh7/Rep-Feo cells were treated with combinations of myriocin and IFN at various concentrations. The relative dose-inhibition curves of IFN were plotted for each fixed concentration of myriocin (0, 30, 100, and 300 nmol/L). As demonstrated in the upper panel of figure 5A, the curves shifted to the left with increasing concentrations of myriocin, demonstrating the synergy of the 2 drugs against the subgenomic HCV-1b replicon. Isobologram analysis also confirmed the synergy (figure 5A, lower panel). To determine whether this synergistic effect was associated with up-regulation of the IFN-stimulated gene responses, we investigated the combined effect of myriocin and IFN on ISRE activity. As demonstrated in figure 5B (upper panel, right), myriocin did not enhance the ISRE-*Renilla* luciferase activity induced by IFN, but

**Figure 2.** Specific inhibition of the replication of a subgenomic hepatitis C virus (HCV) genotype 1b replicon by myriocin. *A*, Inhibition of HCV replicon replication by myriocin. By use of Huh7/Rep-Feo cells expressing a selectable chimeric luciferase reporter Feo gene, the intracellular replication level of an HCV replicon was quantified on the basis of luciferase activity [22, 25]. Huh7/Rep-Feo cells were cultured with various concentrations of myriocin. After 96 h of treatment, the luciferase assay was performed, as described in Materials and Methods (upper panel). In the dimethylthiazol carboxymethoxyphenyl sulfophenyl tetrazolium (MTS) assay, Huh7/Rep-Feo cells were cultured with various concentrations of myriocin for 96 h (lower panel). Data are means  $\pm$  SDs of triplicates from 2 independent experiments. *B*, Northern hybridization. Huh7/Rep-Feo cells were cultured with various concentrations of myriocin and harvested at 96 h after administration. Ten micrograms of total cellular RNA was electrophoresed in each lane. The membrane containing the HCV replicon RNA was hybridized using a digoxigenin-labeled probe specific for the replicon sequence (upper panel), and 28S human ribosomal RNA (rRNA) was used as an internal control (lower panel). Lane 1, no myriocin; lane 2, 300 nmol/L myriocin; lane 3, 1000 nmol/L myriocin. *C*, Western blotting. Ten micrograms of total cellular protein was electrophoresed in each lane. Anti-NSSA monoclonal antibody was used as the primary antibody to detect HCV proteins (upper panel), and  $\beta$ -actin was used as an internal control (lower panel). Lane 1, no myriocin; lane 2, 300 nmol/L myriocin; and lane 3, 1000 nmol/L myriocin. *D*, No enhancement of interferon (IFN)-stimulated response element (ISRE) promoter activity by myriocin. To investigate whether the effect of myriocin was associated with the activation of IFN-stimulated genes, the ISRE-*Renilla* luciferase plasmid was transfected into Huh7/Rep-Feo cells in the presence of myriocin. The upper panel demonstrates the ISRE-*Renilla* luciferase activity at 48 h after transfection. The lower panel demonstrates the firefly luciferase activity of the Huh7/Rep-Feo cells, reflecting HCV replication. Data are means  $\pm$  SDs of triplicates from 2 independent experiments. \* $P < .05$ . *E*, Decrease in the sphingomyelin (SM) content of Huh7 cells after myriocin treatment. The change in the cellular phospholipid content was analyzed by thin-layer chromatography. Huh7 cells were cultured alone or with 100 nmol/L myriocin for 96 h. PC, phosphatidylcholine; PE, phosphatidylethanolamine. *F*, Restoration of the HCV replication that was suppressed by myriocin after the addition of phytosphingosine. Huh7/Rep-Feo cells were cultured with myriocin alone or with various concentrations of phytosphingosine. The luciferase assay was performed after 72 h of treatment (upper panel). Huh7/Rep-Feo cells were also cultured with phytosphingosine alone as indicated for 72 h (lower panel). Data are means  $\pm$  SDs of triplicates from 2 independent experiments. \* $P < .05$ . *G*, Suppression of HCV replication by knocking down of serine palmitoyltransferase (SPT) with short interfering RNA (siRNA). Huh7/Rep-Feo cells were transfected with 10 nmol/L siRNA oligonucleotides targeting the LCB1 subunit of SPT or control siRNA targeting green fluorescent protein (GFP). The luciferase activity of the HCV replicon was measured 72 h after transfection (upper panel). SPT mRNA expression at 72 h after siRNA transfection was analyzed by real-time polymerase chain reaction. The SPT mRNA level was measured relative to 18S rRNA (lower panel). Values are shown as ratios to negative control levels and as the means  $\pm$  SDs of triplicates from 2 independent experiments. siRNA(-), no siRNA. \* $P < .05$ .

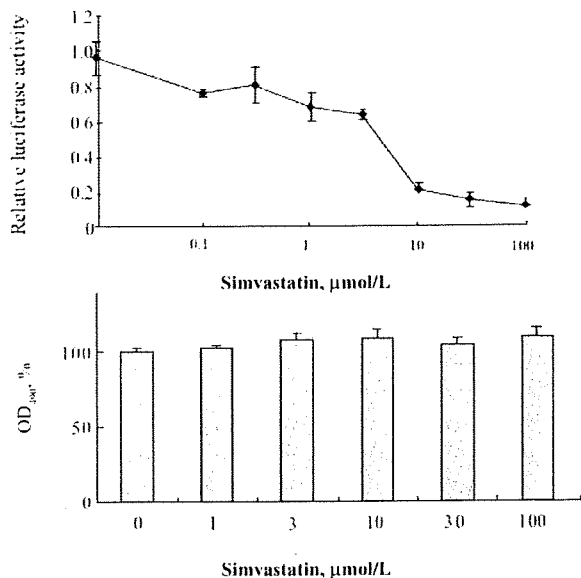


**Figure 3.** Inhibition of replication of a subgenomic hepatitis C virus genotype 1b replicon by simvastatin. Huh7/Rep-Feo cells were cultured with various concentrations of simvastatin, and the luciferase assay was performed after 48 h of treatment (*upper panel*). The dimethylthiazol carboxymethoxyphenyl sulfophenyl tetrazolium assay was performed after Huh7/Rep-Feo cells were cultured with various concentrations of simvastatin for 48 h (*lower panel*). Data are means  $\pm$  SDs of triplicates from 2 independent experiments.

it significantly enhanced IFN-induced suppression of the firefly luciferase activity reflecting HCV replication (*lower panel, right*). This demonstrated that the synergistic effect was not caused by up-regulation of the IFN-stimulated genes. We also assessed the synergy of simvastatin with IFN and of myriocin with simvastatin. In each case, the 2 drugs showed synergistic effects at the concentrations indicated (figure 5C and 5D). In all cases, the MTS reduction values at the drug concentrations used in this assay did not show any significant decrease (data not shown). These results indicate that the synergistic effects on HCV replication of IFN with myriocin, IFN with simvastatin, and myriocin with simvastatin were exerted through their pharmacological effects and were not due to the augmentation of cytotoxicity.

**Suppression of JFH-1 HCV replication by myriocin and simvastatin.** The experiments described thus far were done using the subgenomic HCV-1b replicon system. Recently, Wakita et al. [19] established an infectious HCV model in cultured cells. This system, known as the JFH-1 system and based on genotype 2a HCV, secretes viral particles into the medium, and the medium is infectious for chimpanzees. This JFH-1 system completely mimics HCV infection in vivo and is considered more suitable for analyzing the effect of drugs. Therefore, we

examined the effect of myriocin and simvastatin using the JFH-1 system. Huh7.5.1/JFH-1 HCV cells were cultured for 96 h with 1000 nmol/L myriocin, 10 µmol/L simvastatin, 1000 IU/mL IFN, and a combination of 1000 nmol/L myriocin and 10 µmol/L simvastatin. The intracellular JFH-1 HCV RNA titer was analyzed using real-time RT-PCR. As demonstrated in figure 6A, intracellular JFH-1 HCV RNA treated with myriocin or simvastatin decreased to 60% of control in 96 h, demonstrating that the inhibitory effect of myriocin and simvastatin on replication was not restricted to the subgenomic HCV-1b replicon. When both agents were used in combination, JFH-1 HCV RNA also

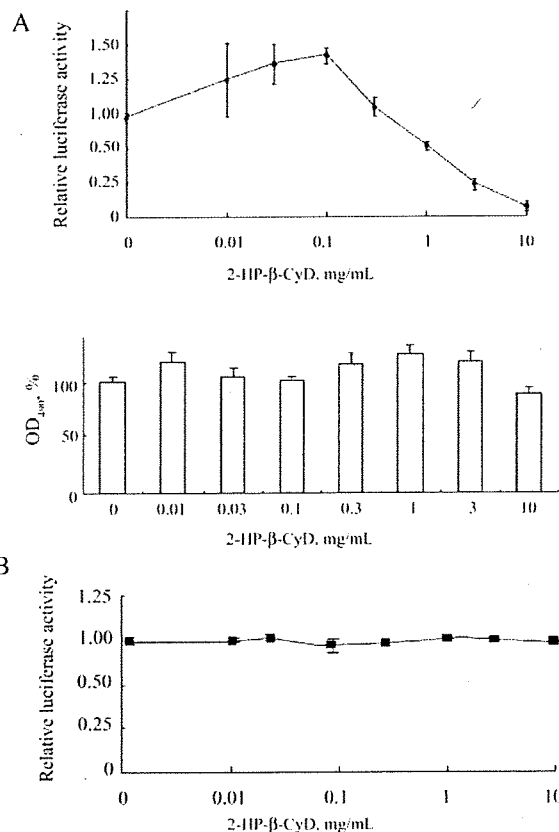


**Figure 4.** Inhibition of replication of a subgenomic hepatitis C virus genotype 1b replicon by 2-hydroxypropyl-β-cyclodextrin (2-HP-β-CyD). A, Huh7/Rep-Feo cells cultured with various concentrations of 2-HP-β-CyD for 48 h. The luciferase assay was performed after 48 h of treatment (*upper panel*). The dimethylthiazol carboxymethoxyphenyl sulfophenyl tetrazolium assay was performed after Huh7/Rep-Feo cells were cultured with various concentrations of 2-HP-β-CyD for 48 h (*lower panel*). Data are means  $\pm$  SDs of triplicates from 2 independent experiments. B, Recombinant firefly luciferase incubated with various concentrations of 2-HP-β-CyD in the culture medium at 37°C for 48 h. The medium was collected and subjected to luciferase analysis. Data are means  $\pm$  SDs of triplicates from 2 independent experiments.

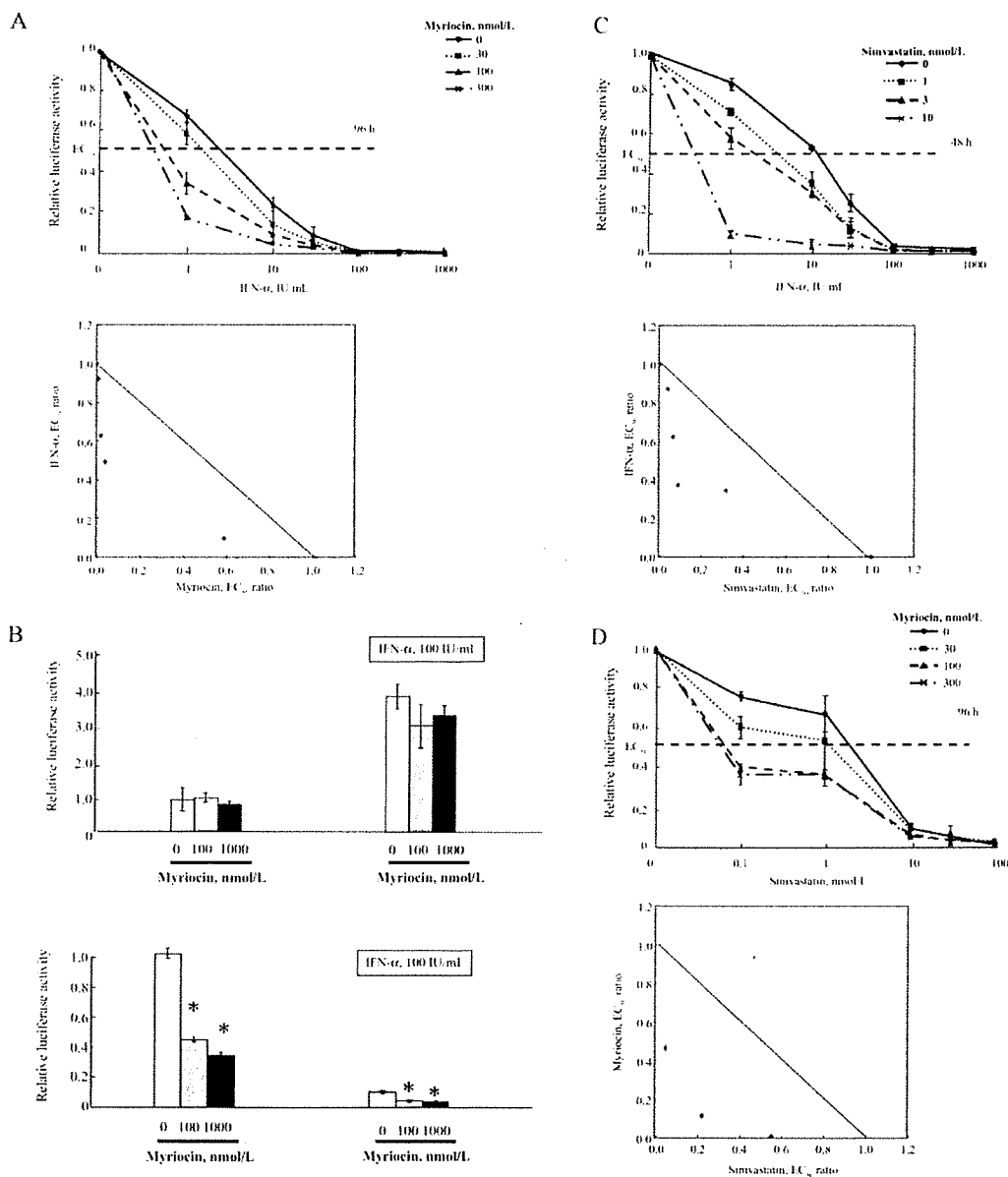


**Figure 5.** Synergistic inhibitory effects of myriocin with interferon (IFN), simvastatin with IFN, and myriocin with simvastatin. *A*, Synergistic inhibitory effect of myriocin with IFN on hepatitis C virus replication. Huh7/Rep-Feo cells were treated with combinations of myriocin and IFN at various concentrations. The upper panel shows the relative dose-inhibition curves of IFN plotted for each fixed concentration of myriocin (0, 30, 100, and 300 nmol/L). The lower panel shows the isobologram analysis for the combination of myriocin with IFN. *B*, IFN-stimulated response element (ISRE) promoter activity induced by a combination of myriocin with IFN. Huh7/Rep-Feo cells transfected with ISRE-*Renilla* luciferase were cultured with various concentrations of myriocin alone (*left*) or with 100 IU/mL IFN (*right*). The upper panel demonstrates the ISRE-*Renilla* luciferase activity at 48 h after transfection. The lower panel demonstrates the firefly luciferase activity of the Huh7/Rep-Feo cells, reflecting hepatitis C virus (HCV). Data are means  $\pm$  SDs of triplicates from 2 independent experiments. \* $P < .05$ . *C*, Synergistic inhibitory effect of simvastatin with IFN on HCV replication. *D*, Synergistic inhibitory effect of simvastatin and myriocin on HCV replication.

decreased to almost 60% of the control at 48 and 96 h after treatment. However, no evident synergistic inhibitory effect was observed (figure 6A). To clarify the inhibitory effect of myriocin on JFH-1 HCV, we performed Western blot analysis for JFH-1

HCV proteins. As demonstrated in figure 6B, a substantial decrease in the core and NS3 proteins of JFH-1 HCV was observed 96 h after treatment with myriocin, confirming the RT-PCR results (figure 6B).

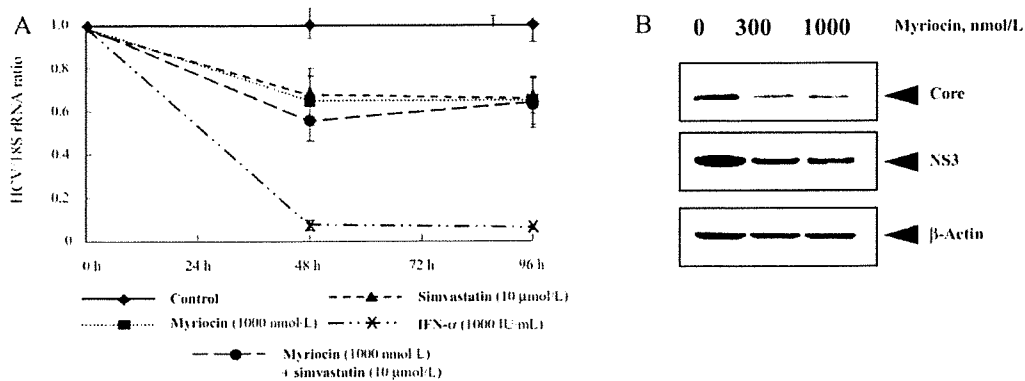


**Figure 6.** Suppression of JFH-1 hepatitis C virus (HCV) replication by myriocin and simvastatin. *A*, Cells containing JFH-1 HCV treated for 96 h with 1000 nmol/L myriocin, 10 μmol/L simvastatin, 1000 IU/mL IFN, or a combination of 1000 nmol/L myriocin and 10 μmol/L simvastatin. The cells were collected at 48 and 96 h, and the JFH-1 HCV RNA level relative to 18S rRNA was analyzed by real-time polymerase chain reaction. Values are shown as the ratios to negative control values (cells receiving no treatment) and as means ± SDs. *B*, Western blotting. Cells containing JFH-1 HCV were treated with 300 or 1000 nmol/L of myriocin and harvested at 96 h after administration. Ten micrograms of total cellular protein was electrophoresed in each lane. Anti-core monoclonal antibody (MAb) and anti-NS3 MAb were used as the primary antibodies to detect JFH-1 HCV proteins. β-Actin was detected as an internal control. Lane 1, no myriocin; lane 2, 300 nmol/L myriocin; and lane 3, 1000 nmol/L myriocin.

## DISCUSSION

In the present study, we demonstrated that the sphingomyelin synthesis inhibitor myriocin suppressed not only replication of a subgenomic HCV-1b replicon but also replication of the JFH-1 strain of infectious genotype 2a HCV. We also demonstrated that simvastatin suppressed replication of both a subgenomic HCV-1b replicon and JFH-1 HCV. When a subgenomic HCV-1b replicon was used, the anti-HCV activity of both myriocin and simvastatin was enhanced synergistically with IFN. Moreover, when myriocin and simvastatin were used together, their anti-HCV activity was enhanced synergistically.

What is the mechanism by which myriocin suppresses viral replication? Because myriocin is a specific inhibitor of SPT, which catalyzes the first committed step of sphingomyelin biosynthesis, we speculated that myriocin exerts its action by inhibiting production of downstream substrates, especially sphingomyelin. The findings that siRNA targeted against SPT decreased HCV replication and that HCV replication was restored by addition of phytosphingosine, a precursor of sphingomyelin, demonstrated that the effect was specific to SPT activity. Moreover, the fact that treatment of Huh7 cells with myriocin did not enhance the ISRE promoter activity indicated that the inhibitory effects of myriocin were independent of those of IFN. It is known that intracellular replication of most RNA viruses occurs on certain membrane structures—including the endoplasmic reticulum, the Golgi apparatus, endosomes, and lysosomes—by making replication complexes at these sites [5–7]. For HCV, it has been reported by several groups that *in vitro* replication activity is located in the membrane fractions of cultured cells [26–28]. In addition, newly synthesized HCV RNA and the nonstructural proteins in replicon cells were colocalized in detergent-resistant

membrane structures, most likely lipid rafts [18]. Caveolin-2, a lipid raft protein, was also shown to colocalize with the nonstructural proteins [18]. According to these findings, the HCV replication complex machinery is considered to form on a lipid raft. Therefore, because sphingomyelin is the major component of the lipid raft, it is plausible to speculate that myriocin disrupted lipid raft formation and inhibited HCV replication.

Cholesterol is another major component of lipid rafts and might also be targeted for anti-HCV therapy. Because cholesterol is synthesized in the mevalonate pathway, an inhibitor of the pathway might act to disrupt lipid rafts. In accordance with this concept, statins, which are HMG-CoA reductase inhibitors, already have been reported to suppress the replication of genomic and subgenomic HCV-1b replicons [15, 16]. In the present study, we also confirmed that simvastatin suppressed replication of a subgenomic HCV-1b replicon without toxicity. Moreover, we showed for the first time that the suppressive effect was also observed in an infectious HCV-2a model of JFH-1 HCV. Meanwhile, recent studies found that the effect of statins was attributable to inhibition of geranylgeranylation rather than depletion of cholesterol, because addition of geranylgeraniol rescued HCV suppression induced by statins [15]. However, although geranylgeranylation might play a role in HCV regulation, the importance of cholesterol itself has not yet been determined. To clarify further the role played by cholesterol in HCV replication, we investigated the effect of 2-HP-β-CyD, which is known to deplete cholesterol directly from cells. As demonstrated in figure 4, specific suppression of HCV replication by 2-HP-β-CyD indicated the importance of cholesterol itself for HCV replication. It is unlikely that these agents suppressed replication of the subgenomic replicon through inhibi-

tion of encephalomyocarditis virus internal ribosome entry site (EMCV-IRES) activity, because they also significantly suppressed replication of a full-length genomic HCV (JFH-1 HCV) that does not include EMCV-IRES (figure 6A; data for 2-HP- $\beta$ -CyD not shown).

Although we observed an inhibitory effect of myriocin and simvastatin on both the subgenomic HCV-1b replicon and JFH-1 HCV, there was a difference in efficacy between the 2 HCV systems; the subgenomic HCV-1b replicon was more sensitive to and was more strongly inhibited by either agent alone or in combination, compared with JFH-1 HCV. This result was unexpected, because we had speculated that these agents might be effective irrespective of the viral isolate if these agents targeted not the virus itself but rather host factors, such as lipid rafts. However, there are several differences between these 2 systems, and we cannot directly compare the results. In particular, the subgenomic HCV replicon lacks viral structural proteins and has only an HCV RNA intracellular replication step, whereas JFH-1 HCV includes all steps of the HCV life cycle. We do not know the precise target of the agents, and further studies are still needed.

Is it really possible to use these agents in clinical HCV treatment? Especially because statins have been used in the treatment of hyperlipidemia for many years worldwide with proven safety, it would be ideal if we could use statins as one therapeutic application for anti-HCV therapy. Most recently, O'Leary et al. [29] undertook a human pilot study and treated 10 patients with atorvastatin for 12 weeks; they reported that there was no statistically significant change in HCV RNA levels compared with pretreatment levels. The reason for the discrepancy between in vitro and in vivo findings is unknown. However, as also discussed by O'Leary et al., the most plausible explanation for this discrepancy is that the plasma concentrations of atorvastatin after a conventionally approved dose were unlikely to reach those found to be effective in cell culture medium. According to their calculations, to inhibit HCV RNA replication the plasma atorvastatin concentration should be 3 logs higher than that achieved by a conventional dose. However, even though it would be difficult to inhibit HCV RNA replication with statins alone, a clinical antiviral effect might be still achieved if statins were used in combination with IFN (or myriocin), because a synergistic effect was observed in our in vitro study. To determine the synergistic effect in vivo, however, further clinical trials are needed. On the other hand, although promising in vitro, myriocin has not yet been used for human clinical diseases, and its safety has not been established. However, in chimeric mice, the plasma myriocin concentration equivalent to culture medium effectively inhibited HCV RNA replication, and drug toxicity was not observed at this concentration [30]. This finding suggested the possibility that myriocin could be used in vivo, although further studies are needed.

In conclusion, we have demonstrated that inhibition of the sphingomyelin synthesis pathway and the mevalonate pathway

both effectively suppressed HCV replication in vitro, indicating that lipid metabolism could be an important target for new anti-HCV therapies.

## References

1. Global surveillance and control of hepatitis C. Report of a WHO consultation organized in collaboration with the Viral Hepatitis Prevention Board, Antwerp, Belgium. *J Viral Hepat* 1999; 6:35–47.
2. Hoofnagle JH. Hepatitis C: the clinical spectrum of disease. *Hepatology* 1997; 26:15S–20S.
3. Seeff LB. Natural history of chronic hepatitis C. *Hepatology* 2002; 36: S35–46.
4. Fried MW, Shiffman ML, Reddy KR, et al. Peginterferon alfa-2a plus ribavirin for chronic hepatitis C virus infection. *N Engl J Med* 2002; 347: 975–82.
5. Wengler G, Nowak T, Castle E. Description of a procedure which allows isolation of viral nonstructural proteins from BHK vertebrate cells infected with the West Nile flavivirus in a state which allows their direct chemical characterization. *Virology* 1990; 177:795–801.
6. Shi ST, Schiller JJ, Kanjanahaluethai A, Baker SC, Oh JW, Lai MM. Colocalization and membrane association of murine hepatitis virus gene 1 products and de novo-synthesized viral RNA in infected cells. *J Virol* 1999; 73:5957–69.
7. van der Meer Y, Snijder EJ, Dobbe JC, et al. Localization of mouse hepatitis virus nonstructural proteins and RNA synthesis indicates a role for late endosomes in viral replication. *J Virol* 1999; 73:7641–57.
8. Ahlquist P, Noueiry AO, Lee WM, Kushner DB, Dye BT. Host factors in positive-strand RNA virus genome replication. *J Virol* 2003; 77:8181–6.
9. Egger D, Wolk B, Gosert R, et al. Expression of hepatitis C virus proteins induces distinct membrane alterations including a candidate viral replication complex. *J Virol* 2002; 76:5974–84.
10. Moradpour D, Gosert R, Egger D, Penin F, Blum HE, Bienz K. Membrane association of hepatitis C virus nonstructural proteins and identification of the membrane alteration that harbors the viral replication complex. *Antiviral Res* 2003; 60:103–9.
11. Gao L, Aizaki H, He JW, Lai MM. Interactions between viral nonstructural proteins and host protein hVAP-33 mediate the formation of hepatitis C virus RNA replication complex on lipid raft. *J Virol* 2004; 78: 3480–8.
12. Aizaki H, Lee KJ, Sung VM, Ishiko H, Lai MM. Characterization of the hepatitis C virus RNA replication complex associated with lipid rafts. *Virology* 2004; 324:450–61.
13. Mannova P, Fang R, Wang H, et al. Modification of host lipid raft proteome upon hepatitis C virus replication. *Mol Cell Proteomics* 2006; 5: 2319–25.
14. Leu GZ, Lin TY, Hsu JT. Anti-HCV activities of selective polyunsaturated fatty acids. *Biochem Biophys Res Commun* 2004; 318:275–80.
15. Kapadia SB, Chisari FV. Hepatitis C virus RNA replication is regulated by host geranylgeranylation and fatty acids. *Proc Natl Acad Sci USA* 2005; 102:2561–6.
16. Ikeda M, Abe K, Yamada M, Dansako H, Naka K, Kato N. Different anti-HCV profiles of statins and their potential for combination therapy with interferon. *Hepatology* 2006; 44:117–25.
17. Sakamoto H, Okamoto K, Aoki M, et al. Host sphingolipid biosynthesis as a target for hepatitis C virus therapy. *Nat Chem Biol* 2005; 1:333–7.
18. Shi ST, Lee KJ, Aizaki H, Hwang SB, Lai MM. Hepatitis C virus RNA replication occurs on a detergent-resistant membrane that cofractionates with caveolin-2. *J Virol* 2003; 77:4160–8.
19. Wakita T, Pietschmann T, Kato T, et al. Production of infectious hepatitis C virus in tissue culture from a cloned viral genome. *Nat Med* 2005; 11:791–6.
20. Zhong J, Gastaminza P, Cheng G, et al. Robust hepatitis C virus infection in vitro. *Proc Natl Acad Sci USA* 2005; 102:9294–9.



21. Nakagawa M, Sakamoto N, Enomoto N, et al. Specific inhibition of hepatitis C virus replication by cyclosporin A. *Biochem Biophys Res Commun* 2004; 313:42–7.
22. Tanabe Y, Sakamoto N, Enomoto N, et al. Synergistic inhibition of intracellular hepatitis C virus replication by combination of ribavirin and interferon- alpha. *J Infect Dis* 2004; 189:1129–39.
23. Bligh EG, Dyer WJ. A rapid method of total lipid extraction and purification. *Can J Biochem Physiol* 1959; 37:911–7.
24. Martell M, Gomez J, Esteban JJ, et al. High-throughput real-time reverse transcription-PCR quantitation of hepatitis C virus RNA. *J Clin Microbiol* 1999; 37:327–32.
25. Yokota T, Sakamoto N, Enomoto N, et al. Inhibition of intracellular hepatitis C virus replication by synthetic and vector-derived small interfering RNAs. *EMBO Rep* 2003; 4:602–8.
26. Schmidt-Mende J, Bieck E, Hugel T, et al. Determinants for membrane association of the hepatitis C virus RNA-dependent RNA polymerase. *J Biol Chem* 2001; 276:44052–63.
27. Pietschmann T, Lohmann V, Rutter G, Kurpanek K, Bartenschlager R. Characterization of cell lines carrying self-replicating hepatitis C virus RNAs. *J Virol* 2001; 75:1252–64.
28. Lai VC, Dempsey S, Lau JY, Hong Z, Zhong W. In vitro RNA replication directed by replicase complexes isolated from the subgenomic replicon cells of hepatitis C virus. *J Virol* 2003; 77:2295–300.
29. O'Leary JG, Chan JL, McMahon CM, Chung RT. Atorvastatin does not exhibit antiviral activity against HCV at conventional doses: a pilot clinical trial. *Hepatology* 2007; 45:895–8.
30. Umehara T, Sudoh M, Yasui F, et al. Serine palmitoyltransferase inhibitor suppresses HCV replication in a mouse model. *Biochem Biophys Res Commun* 2006; 346:67–73.

## Identification of Novel Epoxide Inhibitors of Hepatitis C Virus Replication Using a High-Throughput Screen<sup>∇†§</sup>

Lee F. Peng,<sup>1,2,3‡</sup> Sun Suk Kim,<sup>1,4‡</sup> Sirinya Matchacheep,<sup>2,3</sup> Xiaoguang Lei,<sup>5</sup> Shun Su,<sup>5</sup> Wenyu Lin,<sup>1</sup> Weerawat Runguphan,<sup>2,3</sup> Won-Hyeok Choe,<sup>1</sup> Naoya Sakamoto,<sup>6</sup> Masanori Ikeda,<sup>7</sup> Nobuyuki Kato,<sup>7</sup> Aaron B. Beeler,<sup>5</sup> John A. Porco, Jr.,<sup>5</sup> Stuart L. Schreiber,<sup>2,3,8</sup> and Raymond T. Chung<sup>1\*</sup>

GI Unit, Department of Medicine, Massachusetts General Hospital, 55 Fruit Street, Boston, Massachusetts 02114<sup>1</sup>; Department of Chemistry and Chemical Biology, Harvard University, 12 Oxford Street, Cambridge, Massachusetts 02138<sup>2</sup>; The Broad Institute of Harvard and MIT, 7 Cambridge Center, Cambridge, Massachusetts 02142<sup>3</sup>; Department of Gastroenterology and Hepatology, Gachon University Gil Medical Center, 1198 Guwol-dong, Namdong-gu, Incheon, 405-760 Korea<sup>4</sup>; Department of Chemistry and Center for Chemical Methodology and Library Development (CMLD-BU), Boston University, 590 Commonwealth Avenue, Boston, Massachusetts 02215<sup>5</sup>; Department of Gastroenterology and Hepatology, Tokyo Medical and Dental University, Tokyo, Japan<sup>6</sup>; Department of Molecular Biology, Okayama University Graduate School of Medicine, Dentistry, and Pharmaceutical Sciences, Okayama, Japan<sup>7</sup>; and Howard Hughes Medical Institute, Chevy Chase, Maryland<sup>8</sup>

Received 15 February 2007/Returned for modification 7 May 2007/Accepted 28 July 2007

**Using our high-throughput hepatitis C replicon assay to screen a library of over 8,000 novel diversity-oriented synthesis (DOS) compounds, we identified several novel compounds that regulate hepatitis C virus (HCV) replication, including two libraries of epoxides that inhibit HCV replication (best 50% effective concentration, < 0.5  $\mu$ M). We then synthesized an analog of these compounds with optimized activity.**

Hepatitis C virus (HCV) infects over 170 million people worldwide and frequently leads to cirrhosis, liver failure, and hepatocellular carcinoma (1). Currently, the best therapy for the treatment of chronic hepatitis C is a combination of pegylated interferon and ribavirin, which has suboptimal efficacy and has an unfavorable side effect profile (14). The identification of more-effective and better-tolerated agents is therefore a high priority.

We have recently reported the successful adaptation of the Huh7/Rep-Feo replicon cell line (18) to a high-throughput screening assay system (8). Using this system, we previously screened a library of 2,568 well-known compounds whose biological activity is fully characterized (8). In order to discover novel regulators of HCV replication, we then screened a library of 8,064 diversity-oriented synthesis (DOS) compounds (15, 16). This library, known as the DOS set, is a

TABLE 1. Hits by library from the primary high-throughput screening with the DOS set<sup>a</sup>

Library	Increased luciferase signal hit libraries			Antiviral hit libraries		
	Hits	Members	Reference(s)	Hits	Members	Reference(s) or sources
FPA	11	319	5			
BUCMLD	4	880	10, 17	4	880	10, 17, Fig. 1, Table 2
JMM	4	544	13			
UGISS	1	319	2			
BUCMLD epoxyquinol				12	34	10, 17, Fig. 1 and 2, Table 2
SM				9	27	Fig. 1 and 2, Table 2
SpOx				6	612	6, 12
BEA				3	238	3
ICCB6				3	352	4
YKK				2	281	9
RTE				2	159	19

<sup>a</sup> The total number of compounds which comprise each library is listed in the "Members" columns.

\* Corresponding author. Mailing address: GRJ 825A, GI Unit, Massachusetts General Hospital, Boston, MA 02114. Phone: (617) 724-7562. Fax: (617) 726-5895. E-mail: rtchung@partners.org.

† This publication is dedicated to Yoshito Kishi on the occasion of his 70th birthday.

§ Supplemental material for this article may be found at <http://aac.asm.org/>.

‡ L.F.P. and S.S.K. contributed equally to this project.

∇ Published ahead of print on 6 August 2007.

TABLE 2. Results of secondary screening with antiviral hit compounds from the SM and BUCMLD libraries<sup>a</sup>

Compound name	EC <sub>50</sub>	CC <sub>50</sub>
BUCMLD-B10A11	<0.5 (<0.5–0.5)	19.5 (19.4–22.4)
BUCMLD-B10A3	0.7 (<0.5–5.2)	9.0 (7.1–10.0)
BUCMLD-XL-184	1.4 (0.8–3.9)	>50
BUCMLD-B10A5	1.5 (<0.5–5.4)	39.3 (28.6–>50)
BUCMLD-XL-190	2.5 (<0.5–10)	>50
BUCMLD-B10A1	2.6 (1.0–5.0)	18.0 (15.9–19.5)
SM_A14B5	3.5 (2.7–4.4)	27.1 (18.0–44.6)
BUCMLD-XL-189	3.8 (2.2–7.0)	>50
SM_A6B5_2P100	6.6 (4.0–15.3)	>50
BUCMLD-B10A8	7.0 (0.9–30.0)	>50
BUCMLD-B10A10	7.0 (5.4–30.0)	>50
BUCMLD-B10A14	7.6 (1.0–23.0)	>50
BUCMLD-B10A7	7.75 (1.0–30.0)	35.3 (33.6–36.7)
SM_A4B6_2P123	8.0 (6.3–10.0)	>50
SM_A5B5_2P118	9.1 (2.5–16.7)	>50
SM_A7C2_2P155	12.7 (7.0–24.0)	>50
BUCMLD-B13A2	14.2 (6.4–45.0)	>50
SM_A1B2_1P32	19.6 (11.7–28.2)	>50
SM_A1B5_2P24	19.7 (6.25–50.0)	>50
BUCMLD-B13A1	21.1 (7.5–36.7)	>50
SM_A5B3_2P141	25.7 (18.3–39.8)	>50
SM_A5B2_2P142	26.7 (9.1–50.0)	>50
BUCMLD-NTM-EN2-67A	30.0 (0.7–46.1)	>50
SM_A12B3	>30	>50
BUCMLD-B10A13	42.9 (25.2–59.4)	>50
BUCMLD-XL-130	>100	>50

<sup>a</sup> Note that structure-activity relationship SM library compounds are also included. The EC<sub>50</sub> and 50% cytotoxic concentration (CC<sub>50</sub>) are reported in  $\mu\text{M}$  with 95% confidence intervals in parentheses. A value of <0.5 indicates a concentration of less than 0.5  $\mu\text{M}$ ; >30 indicates a concentration of greater than 30  $\mu\text{M}$ ; >50 indicates a concentration of greater than 50  $\mu\text{M}$ ; and >100 indicates a concentration of greater than 100  $\mu\text{M}$ .

meta-library comprised of DOS libraries from chemists throughout the United States and Canada. Information about the DOS set is available at [http://www.broad.harvard.edu/chembio/platform/screening/compound\\_libraries/index.htm](http://www.broad.harvard.edu/chembio/platform/screening/compound_libraries/index.htm).

The high-throughput primary screen and the secondary validation assays were performed as described in our previous publication (8).

Computational data analysis of the primary screening results was performed as previously described (8) except for the hit criteria. As the characteristics of this data set are different from those generated by our previous screen (8), different threshold values were chosen to assure optimal hit selection. Compounds were considered hits for inhibiting replication if they had a composite Z score of <−2.57 in the reporter gene screen, a reproducibility of >0.9 or <−0.9 in that screen, and a composite Z score of >−2.00 in the cell viability screen. Compounds were considered hits for stimulating luciferase production if they had a composite Z score of >2.50 in the reporter gene screen, a reproducibility of >0.9 or <−0.9 in that screen, and a composite Z score of <1.00 in the cell viability screen.

Full synthetic experimental procedures and spectroscopic data for the SM library compounds discussed in this publication are provided in the supplemental material. The synthesis of the full SM library, including compounds not discussed here, will be the subject of an upcoming report.

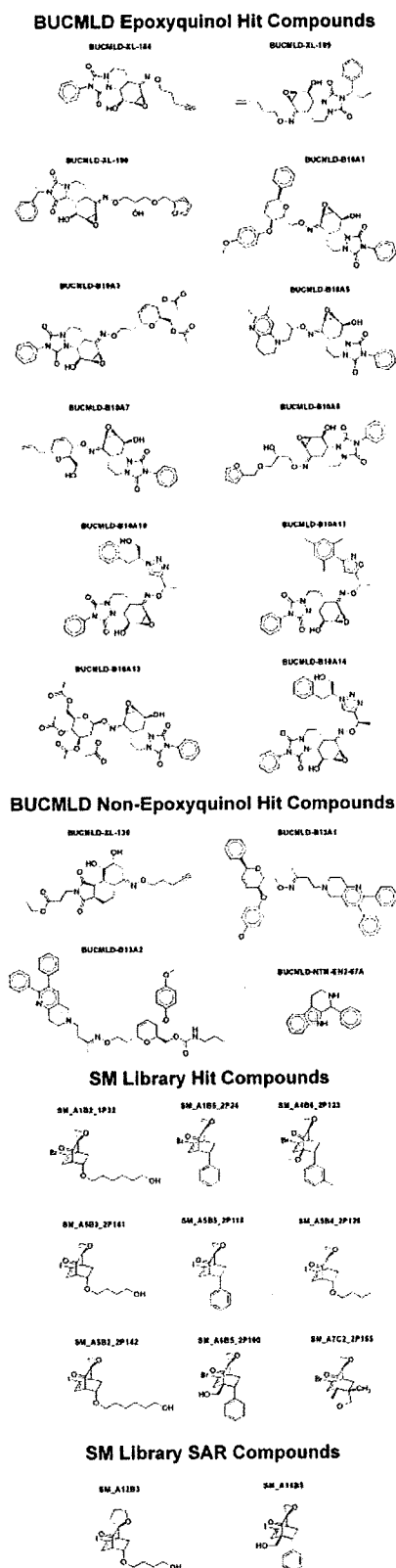


FIG. 1. Structures of antiviral hit compounds from the BUCMLD and SM libraries. SAR, structure-activity relationship.

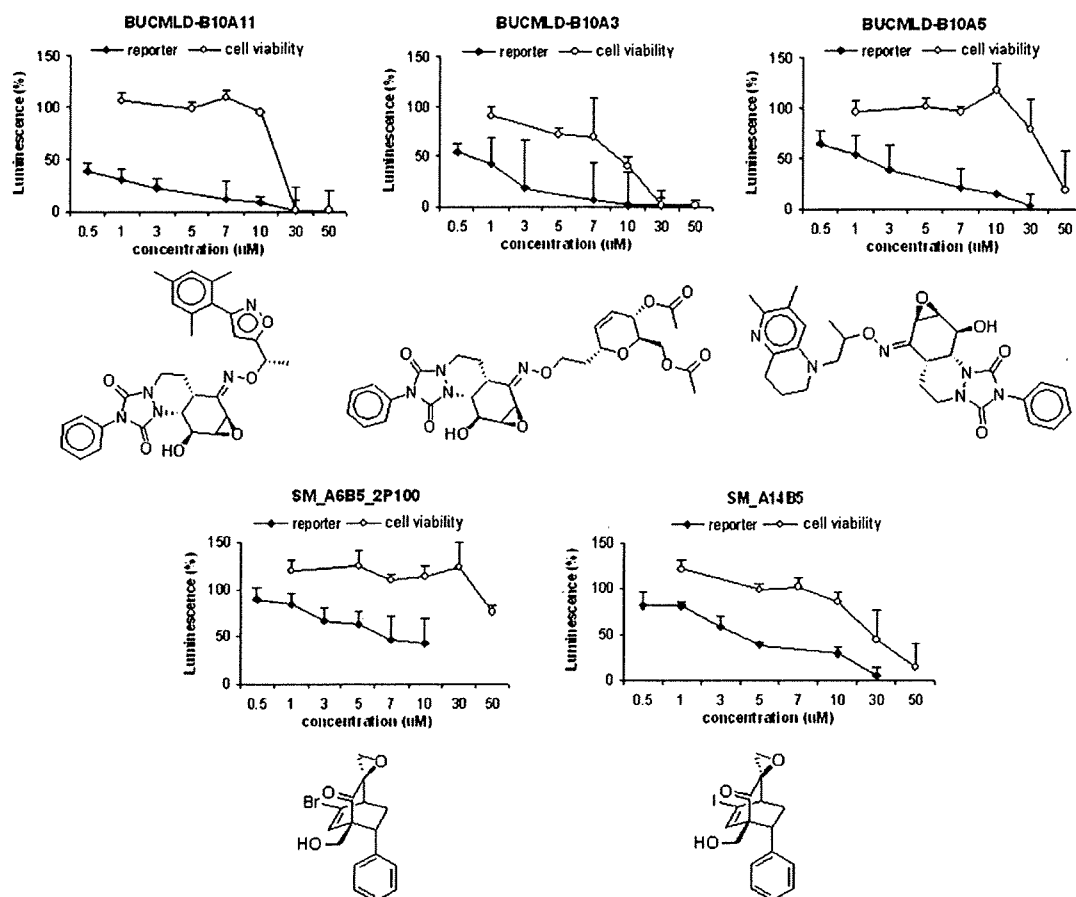


FIG. 2. Selected graphical results of secondary screening with antiviral hit compounds from the SM and BUCMLD epoxyquinol libraries. Luciferase activity for HCV RNA replication levels is shown as a percentage of control. Cell viability is also shown as a percentage of control. Each point represents the average of triplicate data points with standard deviation represented as the error bar.

The synthesis of the BUCMLD epoxyquinol library has been previously described (10, 17).

Full experimental details regarding the JFH1 HCVcc system (11) are provided in the supplemental material. We identified 41 antiviral compounds that inhibited HCV replication and 20 proviral compounds that increased luciferase production (Table 1). In our analysis of the antiviral hit compounds from the DOS set, a striking finding was that 21 of the 41 compounds contained an epoxide moiety. Moreover, the most potent of these compounds were epoxides. Further analysis revealed that these epoxides came from only two DOS libraries, SM and BUCMLD epoxyquinol (10, 17), with very high sublibrary hit rates of 35% and 33%, respectively (Table 1). Of note, the non-hit members of these two libraries did exhibit antiviral activity but failed to meet the formal hit criteria.

As we were especially intrigued by these epoxide-bearing compounds, we restricted our hit validation to these compounds (Table 2 and Fig. 1). SM\_A6B5\_2P100 was the most active member of the SM library, while BUCMLD-B10A11 was the most potent member of the BUCMLD epoxyquinol library (Table 2 and Fig. 2).

Structure-activity relationship analysis of the SM library reveals the structural elements most important for antiviral

activity (Table 2 and Fig. 1). Comparing SM\_A5B5\_2P118 to SM\_A1B5\_2P24, iodinated compounds are more active than brominated ones. Comparing SM\_A5B5\_2P118 to SM\_A5B3\_2P141 and SM\_A5B2\_2P142, compounds with a phenyl substituent are more active than those with aliphatic chains. Finally, the most active compounds, SM\_A4B6\_2P123 and SM\_A6B5\_2P100, have a bridgehead substituent. Thus, we hypothesized that the most active compound should bear an iodine, a phenyl substituent, and a bridgehead substituent.

SM\_A14B5, which incorporates all of these elements, was therefore synthesized, as it was reasoned to be the most active SM library compound. Indeed, SM\_A14B5 had a 50% effective concentration ( $EC_{50}$ ) of approximately 3.5  $\mu$ M, which is about half that of SM\_A6B5\_2P100 (Table 2 and Fig. 2).

The most potent compounds from each library, SM\_A14B5 and BUCMLD-B10A11, underwent further validation in the infectious JFH1 HCVcc system (11). They were tested at concentrations of 5  $\mu$ M and 1  $\mu$ M, respectively, and inhibited HCV replication 48.4%  $\pm$  5.9% and 45.1%  $\pm$  5.2%, respectively, relative to the level of inhibition achieved by interferon at a concentration of 1 ng/ml. These data roughly approximate the  $EC_{50}$  validation data derived from the OR6 system (7) in

which inhibition was also measured relative to that of interferon at a concentration of 1 ng/ml.

Our observations suggest that the epoxide moiety is essential for potent antiviral activity. Analyzing the BUCMLD compounds, those compounds that bear an epoxide moiety are, in general, more-potent antivirals than those that do not (Table 2 and Fig. 1). Furthermore, all of the compounds from the SM library bear epoxides. SM\_A12B3, an analog of SM\_A5B3\_2P141, which bears a tetrahydrofuran moiety in place of an epoxide, was therefore synthesized to further test this hypothesis. SM\_A12B3 had negligible antiviral activity (Table 2), while SM\_A5B3\_2P141 displayed modest antiviral activity. Other analogs of SM compounds bearing tetrahydrofuran rings in place of epoxides showed similar attenuation of antiviral activity relative to their parent compounds. Unfortunately, attempts to synthesize the tetrahydrofuran analog of the most potent SM compound, SM\_A14B5, have so far been unsuccessful.

It is interesting to note that it is the urazole-containing epoxyquinol constituents of the BUCMLD epoxyquinol library, rather than the maleimide-derived ones, that demonstrated anti-HCV activity in the primary screen. It is therefore likely that the combination of a urazole with the epoxide is necessary for the activity of the BUCMLD epoxyquinol compounds.

Although none of our most potent antiviral DOS compounds showed significant cytotoxicity at their  $EC_{50}$ s, all of them ultimately proved to be cytotoxic at higher concentrations (Table 2 and Fig. 2). Therefore, future modifications should not only aim to improve anti-HCV activity but should also attempt to decrease cytotoxicity, in order to widen the therapeutic window.

It is tempting to hypothesize that these epoxides exert their antiviral effects through a common pathway. Presumably, they act as electrophiles, with the nucleophilic target making a covalent bond by attacking and opening the epoxides. Studies to elucidate their mechanism of action are under way.

We thank the National Cancer Institute and the Initiative for Chemical Genetics, who provided support for this publication, and the Chemical Biology Platform of the Broad Institute of Harvard and MIT for their assistance in this work.

The project has been funded in whole or in part with federal funds from the National Cancer Institute's Initiative for Chemical Genetics, National Institutes of Health, under contract no. N01-CO-12400.

The content of this publication does not necessarily reflect the views or policies of the Department of Health and Human Services, nor does mention of trade names, commercial products, or organizations imply endorsement by the U.S. government.

Financial support was provided by the following: The American Gastroenterological Association FDHN/TAP Pharmaceuticals FFT Award (L.F.P.), The GlaxoSmithKline Research Fund of the Korean Association for The Study of The Liver (S.S.K.), NIH ST32DK07191-31 (L.F.P.), NIH NS050854-01 (R.T.C.), and the NIGMS CMLD Initiative P50 GM067041 (J.A.P.).

#### REFERENCES

- Alter, M. J. 2006. Epidemiology of hepatitis C. *Hepatology* 43:S207–S220.
- Andreana, P. R., C. C. Liu, and S. L. Schreiber. 2004. Stereochemical control of the Passerini reaction. *Org. Lett.* 6:4231–4233.
- Brittain, D. E. A., B. L. Gray, and S. L. Schreiber. 2005. From solution-phase to solid-phase enyne metathesis: crossover in the relative performance of two commonly used ruthenium pre-catalysts. *Chem. Eur. J.* 11:5086–5093.
- Burke, M. D., E. M. Berger, and S. L. Schreiber. 2004. A synthesis strategy yielding skeletally diverse small molecules combinatorially. *J. Am. Chem. Soc.* 126:14095–14104.
- Chen, C., X. Li, C. Neumann, M. M.-C. Lo, and S. L. Schreiber. 2005. Convergent diversity-oriented synthesis of small-molecule hybrids. *Angew. Chem.* 117:2–4.
- Chen, C., X. Li, and S. L. Schreiber. 2003. Catalytic asymmetric [3+2] cycloaddition of azomethine ylides. Development of a versatile stepwise, three-component reaction for diversity-oriented synthesis. *J. Am. Chem. Soc.* 125:10174–10175.
- Ikeda, M., K. Abe, H. Dansako, T. Nakamura, K. Naka, and N. Kato. 2005. Efficient replication of a full-length hepatitis C virus genome, strain O, in cell culture, and development of a luciferase reporter system. *Biochem. Biophys. Res. Commun.* 329:1350–1359.
- Kim, S. S., L. F. Peng, W. Lin, W.-H. Choe, N. Sakamoto, S. L. Schreiber, and R. T. Chung. 2007. A cell-based, high-throughput screen for small molecule regulators of HCV replication. *Gastroenterology* 132:311–320.
- Kim, Y.-K., M. A. Arai, T. Arai, J. O. Lamenzo, E. F. Dean, N. Patterson, P. A. Clemons, and S. L. Schreiber. 2004. Relationship of stereochemical and skeletal diversity of small molecules to cellular measurement space. *J. Am. Chem. Soc.* 126:14740–14745.
- Lei, X., N. Zaarur, M. Y. Sherman, and J. A. Porco. 2005. Stereocontrolled synthesis of a complex library via elaboration of angular epoxyquinol scaffolds. *J. Org. Chem.* 70:6474–6483.
- Lindenbach, B. D., M. J. Evans, A. J. Syder, B. Wolk, T. L. Tellinghuisen, C. C. Liu, T. Maruyama, R. O. Hynes, D. R. Burton, J. A. McKeating, and C. M. Rice. 2005. Complete replication of hepatitis C virus in cell culture. *Science* 309:623–626.
- Lo, M. M.-C., C. S. Neumann, S. Nagayama, E. O. Perlstein, and S. L. Schreiber. 2004. A library of spirooxindoles based on a stereoselective three-component coupling reaction. *J. Am. Chem. Soc.* 126:16077–16086.
- Mitchell, J. M., and J. T. Shaw. 2006. A structurally diverse library of polycyclic lactams resulting from systematic placement of proximal functional groups. *Angew. Chem.* 45:1722–1726.
- Pawlotsky, J. M. 1997. Therapy of hepatitis C: from empiricism to eradication. *Hepatology* 26:S62–S65.
- Schreiber, S. L. 2000. Target-oriented and diversity-oriented organic synthesis in drug discovery. *Science* 287:1964–1969.
- Schreiber, S. L. 2003. Chemical genetics. *Chem. Eng. News* 81:51–61.
- Su, S., D. E. Acquilano, J. Arumugasamy, A. B. Beeler, E. L. Eastwood, J. R. Giguere, P. Lan, X. Lei, G. K. Min, A. R. Yeager, Y. Zhou, J. S. Panek, J. K. Snyder, S. E. Schaus, and J. A. Porco. 2005. Convergent synthesis of a complex oxime library using chemical domain shuffling. *Org. Lett.* 7:2751–2754.
- Tanabe, Y., N. Sakamoto, N. Enomoto, M. Kurosaki, E. Ueda, S. Maekawa, T. Yamashiro, M. Nakagawa, C. H. Chen, N. Kanazawa, S. Kakinuma, and M. Watanabe. 2004. Synergistic inhibition of intracellular hepatitis C virus replication by combination of ribavirin and interferon. *J. Infect. Dis.* 189: 1129–1139.
- Taylor, A. M., and S. L. Schreiber. 2006. Enantioselective addition of terminal alkynes to isolated isoquinoline iminiums. *Org. Lett.* 8:143–146.

## A Cell-Based, High-Throughput Screen for Small Molecule Regulators of Hepatitis C Virus Replication

SUN SUK KIM,<sup>\*,‡</sup> LEE F. PENG,<sup>\*,§,||</sup> WENYU LIN,<sup>\*</sup> WON-HYEOK CHOE,<sup>\*</sup> NAOYA SAKAMOTO,<sup>||</sup> STUART L. SCHREIBER,<sup>§,||,#</sup> and RAYMOND T. CHUNG<sup>\*</sup>

<sup>\*</sup>GI Unit, Department of Medicine, Massachusetts General Hospital, Boston Massachusetts; <sup>‡</sup>Department of Gastroenterology and Hepatology, Gachon University Gil Medical Center, Incheon, Korea; <sup>§</sup>Department of Chemistry and Chemical Biology, Harvard University, Cambridge, MA; <sup>||</sup>The Broad Institute of Harvard and MIT, Cambridge, MA; <sup>||</sup>Department of Gastroenterology and Hepatology, Tokyo Medical and Dental University, Tokyo, Japan; <sup>#</sup>Howard Hughes Medical Institute, Chevy Chase, Maryland

**Background & Aims:** Only half of patients with chronic hepatitis C virus (HCV) infection experience sustained virologic response to pegylated-interferon and ribavirin, which cause numerous side effects. Thus, the identification of more effective and better tolerated agents is a high priority. We applied chemical biology to screen small molecules that regulate HCV. **Methods:** We first optimized the Huh7/Rep-Feo replicon cell line for the 384-well microplate format and used this line to screen a large library of well-characterized, known biologically active compounds using automated technology. After identifying several molecules capable of either stimulating or inhibiting HCV replication in this primary screen, we then validated our hit compounds using a full-length HCV replicon cell line in secondary screens. **Results:** We identified and validated a number of antiviral and proviral agents, including HMG-CoA reductase inhibitors (antiviral) and corticosteroids (proviral). The finding of increased replication associated with corticosteroids suggests that these agents directly promote viral replication independent of their suppressive effects on the immune response. The finding of antiviral activity associated with the HMG-CoA reductase inhibitors implies an important role for lipid metabolism in the viral life cycle. **Conclusions:** We have developed a simple, reproducible, and reliable cell-based high-throughput screening assay system using an HCV replicon model to identify small molecules that regulate HCV replication. This method can be used to identify not only putative antiviral agents, but also cellular regulators of viral replication.

Hepatitis C virus (HCV) infects over 170 million people worldwide and frequently leads to cirrhosis, liver failure, and hepatocellular carcinoma.<sup>1</sup> The current best therapy for chronic hepatitis C is a combination of pegylated interferon (PEG-IFN) and ribavirin. Although the sustained virologic response (SVR) rate approaches 80% for patients with genotypes 2 and 3, the SVR rate is limited to about 45% for HCV genotype 1, which is

responsible for about 75% of all cases of HCV in the United States.<sup>2</sup> Furthermore, interferon is parenteral, has an unfavorable side effect profile, and its use requires frequent monitoring for toxicity, ultimately causing 20% of patients to discontinue therapy.<sup>2</sup> The identification of more effective and better tolerated agents is therefore a high priority.

The advancement of our understanding of the mechanisms underlying HCV replication and persistence and the development of new antiviral therapeutics has been hampered by the lack of tractable model systems capable of robust viral replication.<sup>3</sup> However, the recent development of models capable of high-level autonomous HCV RNA replication has greatly facilitated the evaluation of antiviral activities of new anti-HCV drug candidates as well as the study of viral RNA replication and persistence.<sup>4</sup>

In parallel with advances in the cultivation of HCV, chemical biology has emerged as a powerful tool to study biological processes using small organic molecules.<sup>5,6</sup> In the field of chemical biology, 2 general screening approaches have been employed—reverse and forward chemical genetics.<sup>6</sup> Reverse chemical genetics, which has historically been used, starts with a given enzymatic or molecular target and attempts to identify small organic molecules capable of binding to it. The weakness of this approach is that not all binding interactions identified are capable of producing the desired biological effect. On the other hand, forward chemical genetics involves screening perturbagens, such as small molecules, for their effects on a given phenotypic endpoint. All hits, therefore, by definition are biologically meaningful in such a screen. In our case, we were interested in identifying perturbagens capable of modulating HCV replication. Because the level of HCV replication can now be assayed,

**Abbreviations used in this paper:** HCV, hepatitis C virus; HMG-CoA, hydroxyl-methyl-glutaryl coenzyme A; HTS, high-throughput screening; PDE, phosphodiesterase; PEG-IFN, pegylated interferon; S/B, signal-to-background; SVR, sustained virologic response.

© 2007 by the AGA Institute

0016-5085/07/\$32.00

doi:10.1053/j.gastro.2006.10.032

use of the forward chemical genetics approach is now possible.

To efficiently determine whether small molecules exert a certain biological effect in a suitable assay system, rapid high-throughput screening (HTS) methods have been developed. Using the high-density 384-well plate format, it is possible to efficiently and successfully conduct high-throughput phenotypic screens on mammalian cell constructs bearing reporter genes, such as those found in HCV replicon systems, with large libraries of small molecules.<sup>7</sup>

Thus far, however, efficient HTS for HCV drug discovery has remained elusive. Although HCV replicon systems have been established as efficient cell-based screening platforms, no true HTS methods utilizing these systems have been described to date. Experimental barriers have included low signal-to-background ratio and the added burden of complex processing steps, such as washing, aspiration, and lysis prior to signal read-out.

The subgenomic Huh7/Rep-Feo HCV replicon cell line<sup>8</sup> appears to be particularly well suited to automated HTS methods, so it was selected for further assay development. This replicon was derived from a chimpanzee infectious clone (strain HCV-N, genotype 1b). In this replicon, the structural genes have been replaced by a reporter gene. The chimeric reporter gene Feo encodes the firefly luciferase protein fused in-frame with neomycin phosphotransferase. This Huh7/Rep-Feo cell supports high levels of autonomous HCV RNA replication because it was derived from the HCV-N strain, which carries an adaptive mutation in NSSA that confers high-level replication in tissue culture. Furthermore, the level of luciferase correlates well with levels of HCV RNA production, so that luciferase can be used as a reliable surrogate marker for HCV replication. The use of luciferase as a reporter permits quantitative and high-throughput detection of HCV replication levels. The specific use of firefly luciferase makes this replicon especially well-suited for automation, because the luciferase reagent can be added directly to the cell culture system prior to signal detection without the need for cell lysis, washing, or aspiration.

In the course of our attempts to apply chemical biology to the elucidation of the regulation of HCV replication, we first optimized the Huh7/Rep-Feo replicon for the 384-well microplate format and then used it to screen a library of known bioactive compounds using automated technology. After identifying several molecules capable of either stimulating or inhibiting HCV replication in this primary screen, we then validated our hit compounds in secondary screens. Here we describe a simple, reproducible, and reliable cell-based HTS assay system using a HCV replicon model to identify small molecules that regulate HCV replication and further characterize the antiviral properties of the HMG-CoA

reductase inhibitors, as well as the proviral properties of corticosteroids.

## Materials and Methods

### *HCV Replicon System—Primary Screening*

Cells were propagated in Dulbecco's Modified Eagle's medium (DMEM) containing 10% fetal bovine serum (FBS) supplemented with 1% penicillin-streptomycin, and 500  $\mu\text{g}$  of Geneticin (Invitrogen Corp., Carlsbad, CA) /mL. Cells were cultured in a 37°C, 5% CO<sub>2</sub>-humidified incubator for all experiments. To decrease day-to-day variability in the assay, a large homogenous population of subconfluent cells was passaged so that a similar lot of cells could be used throughout the HTS assay.

### *Optimization of Huh-7/Rep-Feo Cells for the 384-Well Plate Format*

The Huh7/Rep-Feo cells were first optimized for the 96-well plate format. Peginterferon-alfa-2b (PEG-Intron; Schering Corp., Kenilworth, NJ) was used as a positive control for inhibition. Cells were seeded at densities of 5000 and 10,000 cells/well in 100  $\mu\text{L}$  of medium in 96-well plates. The cells were allowed to attach overnight (~24 hours) before addition of PEG-IFN at various concentrations (day 0). The plates were then incubated further, and measurements were taken at 24, 48, and 72 hours. At each time point, the plates were equilibrated at room temperature, an equal volume of Bright-Glo reagent (Promega, Madison, WI) was added, and the plates were read in a LumiCount (Packard BioScience Company, Downers Grove, IL) luminometer. For the 384-well plate format, cells were seeded at densities of 1000, 2500, and 5000 cells/well in 30  $\mu\text{L}$  of medium. The remainder of the experiment was carried out as described for 96-well plates. Results were expressed as the mean of 3 replicate wells.

### *Primary Screening—HTS*

Information about the library of known bioactive compounds that was screened and the general automated HTS protocol is available at <http://www.broad.harvard.edu/chembio/index.html>.

Based on the results of optimization experiments in the 384-well plate format, the general HTS protocol was adapted as follows. Unless otherwise indicated, cells were incubated at all times in a humidified environment with 5% CO<sub>2</sub> at 37°C. The assay was initiated by plating 30  $\mu\text{L}$  of medium containing 2000 cells/well into white 384-well opaque-bottom plates (Nunc, Rochester, NY) using an automated plate filler (Bio-Tek  $\mu$ Filler; Winsooki, VT) and allowing the cells to adhere for 24 hours. One hundred nL of compound stock solutions in DMSO was transferred from stock plates into the 384-well assay plates using an automated pin-based compound transfer robot (CyBio CyBi-Well vario; Woburn, MA). The final compound concentration in each well was estimated to be approximately 10–50  $\mu\text{M}$ , with most compounds at 33  $\mu\text{M}$ . The wells

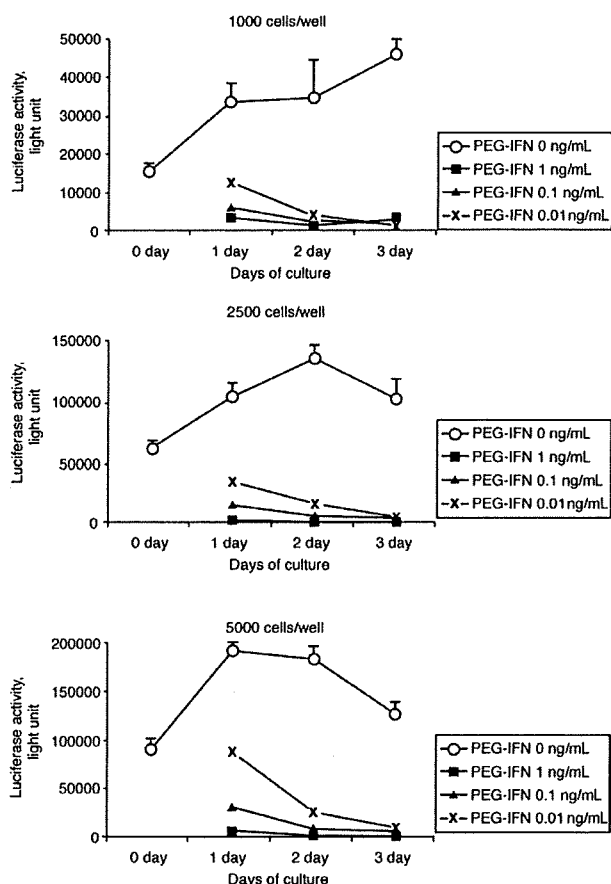


**Figure 1.** Luciferase activity of different cell inoculation concentrations in the 384-well plate format. Different concentrations of PEG-IFN were used as a positive control and to determine signal-to-background (S/B) ratio. HCV RNA replication levels were determined by luciferase activity, as described in Material and Methods. Each point represents the average of 3 data points, with the standard deviation represented as data bars.

contained 0.33% DMSO by volume. The cells were then incubated for another 48 hours. The luminescent signal from each plate was detected using an automated plate reader (Perkin-Elmer Envision 1; Wellesley, MA). This screen was performed in duplicate. For negative controls, entire DMSO-treated control plates were employed, in addition to DMSO-only control wells that were incorporated into each compound assay plate. The cells were assayed for luciferase activity using the Bright-Glo Luciferase assay system (Promega), following the manufacturer's instructions. As a counter-screen, cell viability was assessed using the CellTiterGlo Luminescent cell viability assay (Promega) following the manufacturer's instructions.

#### Computational Data Analysis—Primary Screening

For each replicate, a mock-treatment distribution based on the total population of mock (DMSO) controls in that replicate was built. Each compound was indepen-

dently assigned a sign (ie, "+" or "-") Z-score. Z-scores are calculated by dividing each background-subtracted, compound-treated well by the global standard deviation. A global standard deviation of the background-subtracted, mock-treated wells is calculated over the entire experiment. This distribution was determined to be consistent with experimental noise observed under cell-based assay conditions. The resulting collection of continuous-valued Z-scores represents the primary data set to be used for further analysis. The composite Z-score was calculated as a vector projection of each Z-score in duplicate onto an imaginary line of perfect reproducibility. Reproducibility is the cosine of the angle between each Z-score and that imaginary line; it is dimensionless and ranges from -1 to +1. For analyses dependent upon discrete (ie, binned) outcome states, composite Z-score data were further subjected to a threshold that resulted in each measurement being scored as a high- or low-signal outlier, or as a nonoutlier, from the mock-treatment distribution, based on the possibility that the measurement could be explained by assay noise ( $P_{\text{noise}} < .0005$ ).

The primary data were analyzed using the commercial software packages Pipeline Pilot (SciTegic, San Diego, CA) and SpotFire (SpotFire, Inc., Somerville, MA). The means of the negative, DMSO-only controls were considered the zero point. For the bioactives library, compounds were considered hits for inhibiting replication if they had a composite Z-score of  $< -5.14$  in the reporter gene screen, a reproducibility of  $> 0.9$  or  $< -0.9$  in that screen, and a composite Z-score of  $> -2.57$  in the cell viability screen. Compounds were considered hits for promoting replication if they had a composite Z-score of  $> 5.14$  in the reporter gene screen, a reproducibility of  $> 0.9$  or  $< -0.9$  in that screen, and a composite Z-score of  $< 2.57$  in the cell viability screen.

#### HCV Replicon System—Secondary Assays

For validation, OR6 cells stably harboring the full-length genotype 1 replicon, ORN/C-5B/KE<sup>9</sup> were used to examine compound activity in a more authentic viral polyprotein context. This replicon was derived from the 1B-2 strain (strain HCV-O, genotype 1b), in which the *Renilla* luciferase gene is introduced as a fusion protein with neomycin to facilitate the monitoring of HCV replication. This construct contains a tissue culture adaptive mutation in the NS3 region. Cells were cultured in an identical manner to the Huh7/Rep-Feo cells.

#### Secondary Assays—Hit Validation

Several hits from primary HTS, as well as functionally related compounds, were purchased from Sigma (St. Louis, MO), Calbiochem (San Diego, CA), and Microsource (Gaylordsville, CT). Proviral compounds included (1) corticosteroids—triamcinolone acetonide, prednisolone, dexamethasone, and methylprednisolone, (2) PPAR-gamma ligands—N-(9-fluorenylmethoxy-car-



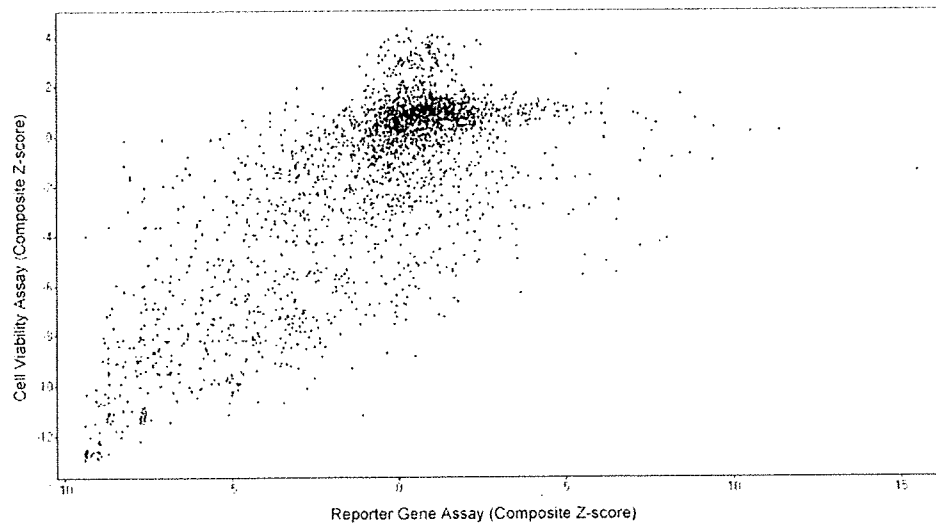


**Figure 2.** A graphical summary of the primary screening for the known bioactives library using Huh7/Rep-Feo cell. Each point represents 1 compound. The X-axis shows HCV replication as measured by normalized luciferase signal, expressed as the composite Z-score. The Y-axis shows cell viability as measured by normalized CellTiterGlo (Promega) signal, expressed as the composite Z-score.

bonyl)-L-leucine (Fmoc-Leu) and troglitazone, and (3) coumarins—marmesin, xanthyletin, dihydro-obliquin, warfarin, coumarin, citrophen, and dicumarol. Antiviral compounds included (1) PDE inhibitors—MY-5445, trequinsin, zaprinast, and rolipram, (2) calcium channel blockers—tetrandrine, verapamil, nifedipine, diltiazem, and nimodipine, (3) MAPK inhibitors—SB-203580, SB-202190, and PD 98059, as well as a negative control (SB 202474), and (4) HMG-CoA reductase inhibitors—atorvastatin, simvastatin, mevastatin, lovastatin, fluvastatin, and pravastatin.

Ten mM of stock solutions of the individual compounds to be tested was prepared in the appropriate solvent (DMSO, ethanol, or H<sub>2</sub>O, according to the manufacturer's information) and stored at -20°C.

Cells were seeded into 96-well plates at a density of 2000 cells/well in 100  $\mu$ L of medium. The cells were incubated for 24 hours at 37°C to obtain the optimal level of adherence. Solutions of candidate hit compounds were added to wells to achieve final concentrations of 0.1, 1, 10, 50, and 100  $\mu$ M. The final concentration of DMSO or ethanol in every well was 1% or less by volume. Mock solutions were used as a negative control. PEG-IFN and ribavirin were used as positive controls at various concentrations, alone and in combination. The plates were then incubated at 37°C with 5% CO<sub>2</sub> for 48 hours before they were analyzed. Luminescent signal was generated using the *Renilla* luciferase assay kit (Promega) according to the manufacturer's instructions. Signal was then detected using a LumiCount (Packard BioScience Company) luminometer. Cell viability was assessed using CellTiter-Glo (Promega), following the manufacturer's instructions. All experiments were performed in triplicate.

### Secondary Assays—Data Analysis

Values were presented as a percentage of mock treated control, which was arbitrarily set at 100%. Data were expressed as the mean  $\pm$  SD. Results were analyzed using a paired *t* test to determine the significance of observed differences between the values of control and individual concentrations and were considered significant if the *P* values were less than .05. Synergy calculations were performed using CalcuSyn (Biosoft; Cambridge, England).

### Results

#### Optimization of Huh-7/Rep-Feo Cells for the 384-Well Plate Format

HCV replication in the subgenomic replicon cell model was tightly coupled to host cell growth conditions.<sup>10,11</sup> Experimentally, HCV RNA replication in the subgenomic replicon cell increased progressively over time, followed by a sharp decline when the cells reached 70% confluence. There was a good linear relationship between cell number and luciferase signal in test tube (data not shown). Inasmuch as the wells of microplates have a small culturable surface, the Huh7/Rep-Feo cells were optimized for both the 96-well and 384-well plate formats using PEG-IFN as a positive control. For 96-well plates, the signal-to-background (S/B) ratio was very high (over 100) when cells were incubated at a concentration of 5000 cells/well at culture day 0. The S/B ratio progressively increased over time, peaking at culture day 2 and then decreased from culture day 3 onward, when cells reached over 70% confluence. The antiviral activity of PEG-IFN progressively increased over time. On the other hand, although the initial S/B ratio at an inoculation

**Table 1.** Hits From the Primary HTS With the Known Bioactives Library

Compound name	R-CompZ	C-CompZ
Proviral hit compounds		
Diphenylurea	15.510	-1.415
Piceid	11.366	0.220
Iridin	10.529	0.162
Biochanin A diacetate	9.416	0.340
5,4'-dimethoxyflavone	9.391	-0.997
Chlorpropham	8.891	0.694
Tectorigenin	8.728	-0.737
N-(9-fluorenylmethoxycarbonyl)-L-leucine	8.440	1.676
7,4'-dimethoxyisoflavone	8.178	-0.852
Dihydro-obliquin	7.825	-1.676
Marmesin	7.700	0.502
Salicylanilide	7.562	0.169
Liquiritigenin dimethyl ether	7.417	0.654
Robustic acid	7.345	-0.546
3,7-dihydroxyflavone	7.226	-1.033
Methimazole	7.169	0.859
Collistimethate	7.040	0.885
Acacetin	6.278	1.846
6,4'-dimethoxyflavone	6.189	0.482
2-ethoxycarbonyl-2-hydroxy-5,7-dimethoxyisoflavanone	6.177	-0.085
Estrone	6.100	0.842
Fenspiride	6.088	1.234
Butirosin A	5.787	0.894
Xanthyletin	5.747	-1.589
Todralazine	5.653	1.222
Niflumic acid	5.297	-1.695
Triamcinolone	5.275	0.703
Cuneatin methyl ether	5.146	0.468
Antiviral hit compounds		
SB-203580	-8.244	-1.160
MY-5445	-8.237	-0.190
Swainsonine	-8.058	-1.577
Pifithrin	-8.043	-1.725
3-alpha-hydroxydeoxygedinlin	-7.701	-2.563
(S)-propranolol	-7.629	-2.439
Andrographolide	-7.618	-2.064
Tetrandrine	-7.091	-0.134
Pregnenolone 16-alpha carbonitrile	-7.059	-1.994
Cyclopamine	-6.766	-2.005
Derrusnin	-6.642	-1.558
2,3,29-triacetoxy-24-nor-1,3,5,7-friedelatetraene	-6.474	-1.734
Atorvastatin	-6.385	-1.259
Coenzyme B-12	-6.300	-0.809
E-64-D	-6.252	-1.502
Deoxyandrobin lactone	-5.839	-2.412
3-beta-hydroxydeoxydesacetoxyl-7-oxogedunin	-5.634	-0.128
U-37883A	-5.527	-1.749
Alachlor	-5.344	-0.075
Veratridine	-5.246	-0.415
1,2-alpha-epoxydeacetyl-dihydrogedunin	-5.177	-2.414

R-CompZ, composite Z-score for reporter gene assay; C-CompZ, composite Z-score for cell viability assay.

concentration of 10,000 cells/well was higher than at 5000 cells/well, there was no significant increase of the S/B ratio over time (data not shown). For 384-well plates, the S/B ratio at an inoculation concentration of 1000

cells/well progressively increased over time, with a large standard deviation. The S/B ratio at an inoculation concentration of 5000 cells/well peaked at culture day 1, when an optimum level of confluence was reached. The S/B ratio at an inoculation concentration of 2500 cells/well was ideal, with the optimal S/B ratio achieved at culture day 2 (Figure 1). We therefore selected 2500 cells/well at culture day 2 for subsequent studies.

### Primary Screening (HTS) Results

Figure 2 shows a graphical representation of the primary HTS results. Many compounds appeared to have strong antiviral activity when the luciferase reporter gene assay alone was considered. When these results were analyzed in conjunction with those of the cell viability assay, however, most of the potential antiviral hit compounds were cytotoxic and, therefore, false positives. For that reason, it is imperative to perform the primary HTS as a 2-dimensional assay with both the level of HCV replication and cell viability measurements, in order to minimize confounding from increased luciferase signals due to increased cell titer and decreased luciferase signals due to decreased cell titer.

Using the data analysis and hit selection criteria outlined in Materials and Methods, we identified 21 antiviral compounds that inhibited HCV replication and 28 proviral compounds that increased HCV replication (Table 1). The respective hit rates of 0.8% and 1.1% are consistent with hit rates for other biological screens performed using this library.

Proviral compounds included steroids (estrone, triamcinolone), coumarins (xanthyletin, dihydrobiquin, and marmesin), flavones, and a PPAR-gamma ligand (N-9-fluorenylmethoxycarbonyl-L-leucine). Antiviral compounds included an HMG-CoA reductase inhibitor (atorvastatin), a beta-adrenergic blocker (propranolol), a calcium channel blocker (tetrandrine), a phosphodiesterase (PDE) inhibitor (MY-5445), and a p38 MAP kinase inhibitor (SB 203580). The finding of antiviral activity associated with the HMG-CoA reductase inhibitor was of particular interest, as the HMG-CoA reductase inhibitor lovastatin has recently been shown to exhibit anti-HCV activity.<sup>12</sup> Although corticosteroids have been assumed to increase HCV replication by means of host immunosuppression, they have not been reported to be a specific proviral agent for HCV independent of their general immunosuppressive activity.<sup>13</sup> SB-203580 has been previously reported to have mixed effects on HCV replication.<sup>14,15</sup>

### Anti-HCV Activity of PEG-IFN and Ribavirin in the OR6 Replicon System

We tested PEG-IFN and ribavirin at various concentrations, alone and in combination, as it has been reported that OR6 cells bearing a genome-length HCV RNA replicon were sensitive to these agents.<sup>9</sup> The IC<sub>50</sub> of

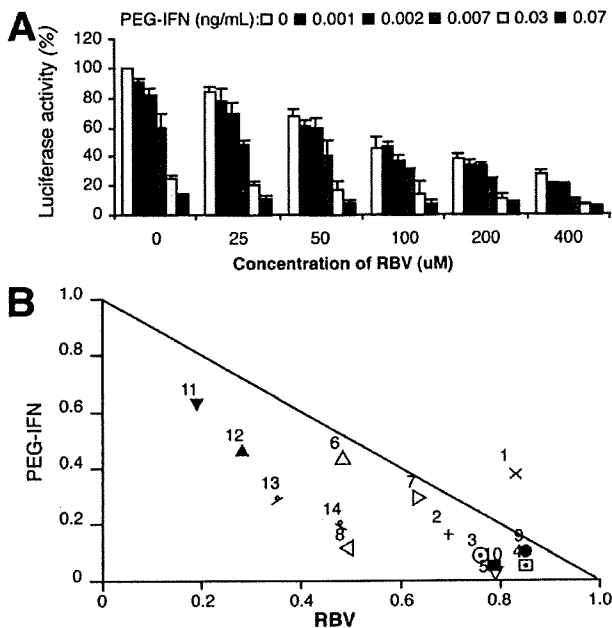


**Figure 3.** (A) Anti-HCV activity of PEG-IFN and ribavirin on HCV RNA replication in OR6 cell system. OR6 cells were cotreated with PEG-IFN (0, 0.001, 0.002, 0.007, 0.03, and 0.07 ng/mL) and ribavirin (0, 25, 50, 100, 200, and 400  $\mu$ M) for 48 hours. Luciferase activity for HCV RNA replication levels is shown as a percentage of control. Each bar represents the average of triplicate data points with standard deviation represented as the error bar. (B) A normalized isobologram generated by CalcuSyn using the data from Figure 3A. Points below and to the left of the line represent synergy. Thirteen of the 14 concentration ratios examined demonstrate the synergistic effect of the combination of PEG-IFN and ribavirin.

PEG-IFN was between 0.007 and 0.03 ng/mL. The  $IC_{50}$  of ribavirin was between 50  $\mu$ M and 100  $\mu$ M (Figure 3A). As previously reported, the combination of ribavirin with PEG-IFN showed synergy (Figure 3B). These results demonstrate that HCV RNA replication in OR6 cells is highly sensitive to PEG-IFN, ribavirin, and a combination of both agents.

#### Hit Validation

Several proviral and antiviral hit compounds identified in the primary screen were selected for further validation on the basis of commercial availability and clinical interest. In order to examine compound activity in a more authentic viral polyprotein context, the validation assays were carried out using the OR6 full-length genotype 1b replicon. Multiple concentrations of each compound were used in order to generate an adequate dose-response curve. In addition to the actual hit compounds themselves, other compounds from the relevant compound classes were subjected to secondary validation assays.

**Proviral compounds.** Triamcinolone was confirmed to increase HCV replication in the full-length HCV replicon system (Figures 4A and B). Other cortico-

steroids (prednisolone, dexamethasone, and methylprednisolone) also increased HCV replication (Figures 4A and B). The PPAR gamma ligand, N-(9-fluorenylmethoxycarbonyl)-L-leucine, which was identified as a proviral hit in the primary screen, showed mild proviral activity. Troglitazone showed proviral activity at 1 and 10  $\mu$ M. The decreased luciferase signal at 50  $\mu$ M and above was due to cytotoxicity. Clofibrate, a PPAR alpha ligand, did not show a proviral effect. The coumarin compounds did not demonstrate any significant proviral activity (data not shown).

**Antiviral compounds.** Although the PDE inhibitor, MY5445, decreased the luciferase signal in a dose-related manner, it displayed significant cytotoxicity. Another PDE inhibitor in the bioactives library, trequinsin, was not identified as a hit in the primary screen, where it was tested at a concentration of 33  $\mu$ M and found to be cytotoxic. It did, however, display antiviral activity at the lower concentrations of 1 and 10  $\mu$ M in the validation assay, with significant cytotoxicity only at the higher concentrations of 50 and 100  $\mu$ M (Figures 5A and B).

The p38 MAPK inhibitor, SB 203580, exhibited antiviral activity at a concentration of 10  $\mu$ M and cytotoxicity at higher concentrations (Figures 5C and D). Other MAPK inhibitors, such as SB 202109, were inactive in both the primary screen and in the secondary assay (data not shown).

The antiviral effect of the calcium channel blocker, tetrandrine, could not be evaluated because of cytotoxicity in the secondary assay (Figures 5E and F). Other

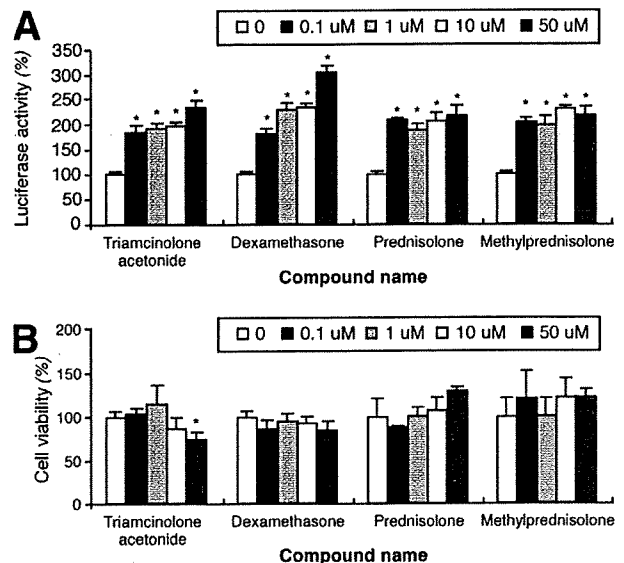


**Figure 4.** Results of secondary screening with corticosteroids. (A) Luciferase activity for HCV RNA replication levels is shown as a percentage of control. (B) Cell viability is also shown as a percentage of control. Each bar represents the average of triplicate data points with standard deviation represented as the error bar. \*Denotes a significant difference from control of at least  $P < .05$ .

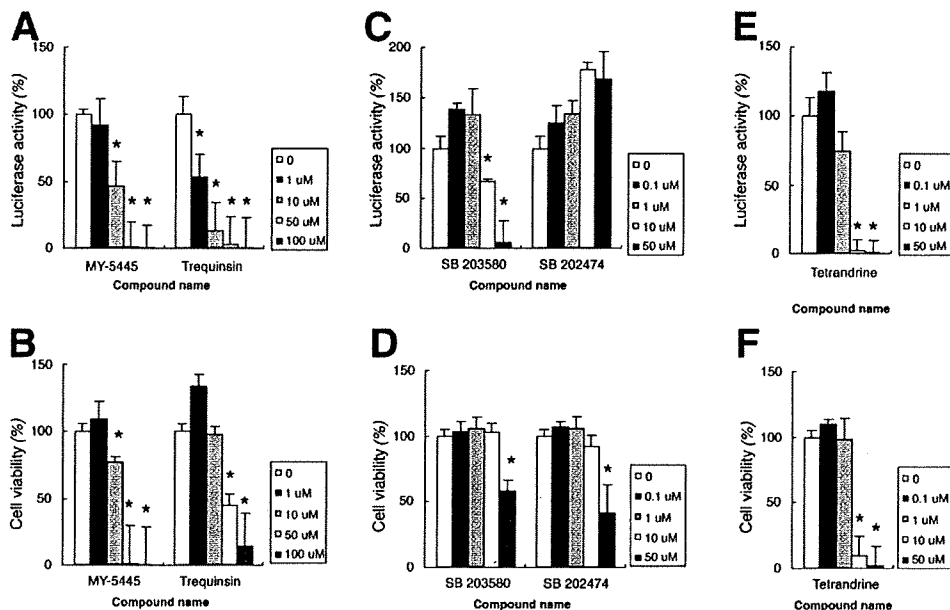


**Figure 5.** Results of secondary screening with several hit compounds. Luciferase activity for HCV RNA replication levels is shown as a percentage of control (A, C, E). Cell viability is also shown as a percentage of control (B, D, F). Each bar represents the average of triplicate data points with standard deviation represented as the error bar. (A, B) MY-5445 and trequinsin (C, D) SB 203580 (E, F) tetrandrine. \*Denotes a significant difference from control of at least  $P < .05$ .

calcium channel blockers, such as verapamil and nifedipine, did not exhibit antiviral activity in either the primary screen or the validation assay (data not shown).

Strikingly, each of the HMG-CoA reductase inhibitors, except for pravastatin, significantly decreased HCV replication in a dose-related manner, with  $\text{IC}_{50}$  values between 1 and 10  $\mu\text{M}$ . Atorvastatin, simvastatin, and fluvastatin

demonstrated strong antiviral effects. Lovastatin, previously reported as an inhibitor of HCV replication,<sup>12</sup> and mevastatin were weakly inhibitory. Lovastatin was significantly cytotoxic at 10, 50, and 100  $\mu\text{M}$ . Mevastatin was not cytotoxic. Pravastatin showed very weak antiviral activity, with only 30% inhibition at 100  $\mu\text{M}$  (Figure 6).

### Discussion

Using a subgenomic HCV replicon model, we have established a rapid, reliable, and reproducible cell-based HTS assay system to identify regulators of HCV replication. After first identifying several bioactive small molecules capable of modulating HCV replication in the primary HTS, we verified these hit compounds using a full-length replicon cell line in the secondary validation assay. This method represents an efficient system for the detection of novel compounds, applicable for both academic and pharmaceutical purposes.

In order to successfully develop and execute an efficient, rapid, and reproducible cell-based HTS assay in the field of anti-HCV drug discovery, one must have access to (1) a high-density, automated screening technology platform, (2) a large and diverse collection of appropriate perturbagens, and (3) an accurate and reliable reporter system, which, in this case, was an HCV replicon line that replicates at high levels and harbors a tractable reporter gene.

Traditional HTS techniques using a 96-well plate have been shown to be less efficient at screening very large libraries than more high-density formats. Moreover,

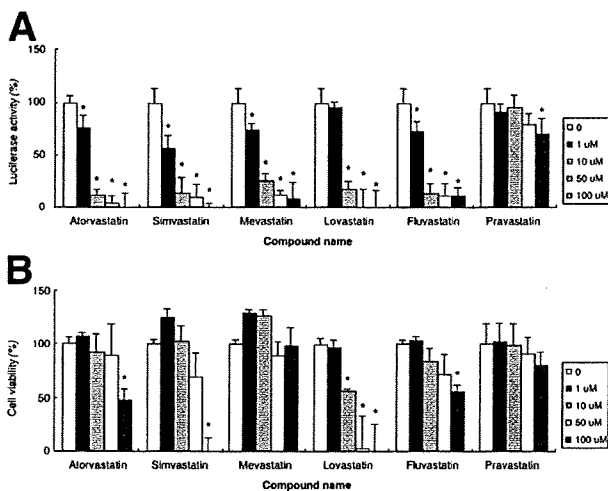


**Figure 6.** Results of secondary screening with the statins. (A) Luciferase activity for HCV RNA replication levels is shown as a percentage of control. (B) Cell viability is shown as a percentage of control. Each bar represents the average of triplicate data points with standard deviation represented as the error bar. \*Denotes significant difference from control of at least  $P < .05$ .